



## Can Color Be Seen in Deep-Inelastic Scattering?\*

SEKAZI K. MTINGWA

Fermi National Accelerator Laboratory<sup>†</sup>  
P.O. Box 500, Batavia, Illinois 60510 (USA)

and

Center for Theoretical Physics, Department of Physics and Astronomy  
University of Maryland, College Park, Maryland 20742 (USA)

and

MURAT ÖZER

Department of Physics and Astronomy, University of Maryland  
College Park, Maryland 20742 (USA)

*November 1980*

### ABSTRACT

We discuss those aspects of the Pati-Salam grand unification scheme which are relevant to deep-inelastic lepton-nucleon scattering. The naive lowest order parton model with massless quarks and massive gluons is presented, and we calculate higher order corrections to the parton distribution functions above the threshold for color production using a covariant formulation of the Altarelli-Parisi program. Below the threshold for color production, we add charm distribution functions to the Owens-Reya parton distributions and get good agreement with the data up to  $Q^2 \sim 100 \text{ GeV}^2$ . Above color threshold, we calculate in detail what effect color production would have on the nucleon isoscalar structure function  $F_2$  to leading nontrivial order in Pati-Salam QCD with massive gluons. Finally, we comment on the present status of experimental attempts to see color in deep-inelastic scattering.

\* Work supported in part by the University of Maryland Computer Science Center, the Ford Foundation, and the National Science Foundation.

<sup>†</sup> Present address.



## I. INTRODUCTION

For some time now there has been considerable interest in testing the standard massless gluon quantum chromodynamics (QCD) model of the strong interactions.<sup>1,2</sup> Recently, Ball et al.<sup>3</sup> generated some excitement when they reported an anomalously large increase in the isoscalar nucleon structure function  $F_2(x, Q^2)$  in deep-inelastic muon-nucleon scattering. Lehman<sup>4</sup> and Özer and Pati<sup>5</sup> have interpreted this anomalous rise in  $F_2$  as due to the excitation of color hadronic final states. Other experimental groups<sup>6</sup> have tried with no success to observe this effect seen by Ball et al.; however, we shall point out below what the kinematic region is which such experiments should exhaust before ruling out entirely the possibility of observing color in deep-inelastic scattering.

The Pati-Salam theory<sup>7</sup> is only one scenario for unifying the strong, weak, and electromagnetic interactions. But any such scheme starts with the minimal gauge group

$$\mathcal{G} = SU(3)^C \otimes SU(2) \otimes U(1) \quad , \quad (1.1)$$

where  $SU(3)^C$  corresponds to the strong interactions and  $SU(2) \otimes U(1)$  to the theory<sup>8,9</sup> of the weak and electromagnetic interactions. Leptons lie in  $SU(3)^C$  singlets and quarks in  $SU(3)^C$  triplets. Moreover, lefthanded quarks and leptons belong to doublets under weak  $SU(2)$  whereas righthanded quarks and leptons belong to weak  $SU(2)$  singlets. All the fermions in the theory occur in generations based upon their masses:

$$\left( \begin{array}{c|ccc} \nu_e & u_r & u_y & u_b \\ e^- & d_r & d_y & d_b \end{array} \right) \left( \begin{array}{c|ccc} \nu_\mu & c_r & c_y & c_b \\ \mu^- & s_r & s_y & s_b \end{array} \right) \left( \begin{array}{c|ccc} \nu_\tau & t_r & t_y & t_b \\ \tau^- & b_r & b_y & b_b \end{array} \right) \quad ,$$

where the three colors are denoted by red (r), yellow (y), and blue (b). This mass hierarchy is as yet poorly understood.

In the SU(5) unification scheme of Georgi and Glashow<sup>10</sup> SU(5) breaks down to  $SU(3)^C \otimes SU(2) \otimes U(1)$  at a mass scale of the order of  $10^{15}$  GeV and this group subsequently breaks down to  $SU(3)^C \otimes U(1)$  at a mass scale of the order of  $10^2$  GeV. Each fermion generation lies in an SU(5) reducible representation  $\bar{5} \oplus 10$ , where the  $SU(3)^C \otimes SU(2)$  decompositions of 5 and 10 are as follows:

$$5 = (1^C, 2) \oplus (3^C, 1) \quad (1.2a)$$

$$10 = (1^C, 1) \oplus (3^C, 2) \oplus (\bar{3}^C, 1) \quad , \quad (1.2b)$$

with the 10-representation being the antisymmetrized product of two 5's. Then, for the first fermion generation we have

$$\bar{5} = \left( \begin{array}{c|c} \nu_e & \bar{d} \\ \hline e^- & \end{array} \right) \quad (1.3a)$$

$$10 = \left( \begin{array}{c|c} u & \bar{u}, e^+ \\ \hline d & \end{array} \right) \quad , \quad (1.3b)$$

and similarly for the other generations. The SU(5) 24-representation for the gauge bosons transforms under  $SU(3)^C \otimes SU(2)$  as follows:

$$24 = (8^C, 1) \oplus (1^C, 3) \oplus (1^C, 1) \oplus (3^C, 2) \oplus (\bar{3}^C, 2) \quad (1.4)$$

where  $(8^C, 1)$  corresponds to the eight massless gluons mediating the strong interactions,  $(1^C, 3) \oplus (1^C, 1)$  corresponds to the weak and electromagnetic  $\gamma, Z, W$ 's, and  $(3^C, 2) \oplus (\bar{3}^C, 2)$  corresponds to the 12 superheavy weak doublet and color triplet

$$\begin{pmatrix} X^c \\ Y^c \end{pmatrix} + \text{antiparticles}$$

whose masses are  $\approx 10^{15}$  GeV and which couple to diquarks and leptoquarks, thus leading to the decay of the proton.

In this massless gluon scheme, the scaling behavior of the structure functions in deep-inelastic lepton-nucleon ( $\ell N$ ) scattering has been worked out some time ago by various authors.<sup>1,2,11</sup> However, a more useful phenomenological approach is obtained if one writes the structure function  $F_2^{\ell N}$  from the lowest order simple parton picture in terms of quark distribution functions as follows:

$$F_2^{\ell N}(x) = \sum_i e_i^2 x [q_i(x) + \bar{q}_i(x)] \quad ,^{12} \quad (1.5)$$

where  $q_i(x)$  and  $\bar{q}_i(x)$  measure the probability for finding a parton of type  $i$  with momentum fraction  $x$  of the parent nucleon and  $e_i$  is the charge of the  $i$ th parton. One then includes the higher order  $Q^2$  corrections to  $F_2^{\ell N}$  by replacing the  $q_i(x)$  and  $\bar{q}_i(x)$  in Eq. (1.5) by their  $Q^2$ -dependent solutions obtained from the Altarelli-Parisi equations.<sup>13</sup> It is this approach which we apply to the Pati-Salam model.

In the next section we review the most important features of the Pati-Salam model necessary for a thorough discussion of deep-inelastic scattering. Comparisons are made to the  $SU(5)$  unification scheme described above. In Sec. III we describe the lowest order parton model description of  $\ell N$  deep-inelastic scattering. In Sec. IV, we calculate the parton transition functions necessary for calculating the higher order corrections to the parton distribution functions above the threshold for color production. In Sec. V we discuss the phenomenology of deep-inelastic scattering below the threshold for color production, adding charm distribution functions to the Owens-Reya parton distribution functions.<sup>14</sup>

Comparisons are made to recent experimental data. In Sec. VI, we use the parton transition functions derived in Sec. IV to calculate the  $Q^2$  dependence of the gluon distribution inside the nucleon. The main results are discussed in Section VII. We choose various values for the color threshold mass  $M_{\text{col}}$  and graph the percentage increase in  $F_2^{\ell N}$  due to the color contribution to the structure function for various values of  $x$ . In addition we discuss the results of Ball et al.<sup>3</sup> Finally, in Section VIII we discuss our results and offer some concluding remarks.

## II. THE PATI-SALAM THEORY<sup>7,15,16</sup>

In this section, we review those aspects of the Pati-Salam theory which are important for the following sections' discussions of deep-inelastic scattering. As for the SU(5) scheme, we again start with the minimal gauge group necessary for describing the strong, weak, and electromagnetic interactions:

$$G_{\text{min}} = \text{SU}(3)_{L+R}^C \otimes \text{SU}(2)_L \otimes \text{U}(1) \quad , \quad (2.1)$$

where L and R denote left and righthandedness. We embed  $G_{\text{min}}$  inside

$$G = [\text{SU}(4)_L \otimes \text{SU}(4)_R]^{\text{color}} \otimes [\text{SU}(4)_L \otimes \text{SU}(4)_R]^{\text{flavor}} \equiv [\text{SU}(4)]^4 \quad . \quad (2.2)$$

This is called chiral color gauging and leads to interesting possibilities as we shall see shortly. There are four independent coupling constants, one corresponding to each SU(4) subgroup; therefore, to reduce that number to one coupling constant  $g_G$  we impose the discrete symmetries

flavor ↔ color

left ↔ right

The basic fermion multiplet--where for our purposes we can ignore the t and b quarks--is as follows:<sup>17</sup>

$$F_{L,R} = \begin{bmatrix} p_r & p_y & p_b & p_\ell = \nu_e \\ n_r & n_y & n_b & n_\ell = e^- \\ \lambda_r & \lambda_y & \lambda_b & \lambda_\ell = \mu^- \\ c_r & c_y & c_b & c_\ell = \nu_\mu \end{bmatrix}_{L,R}, \quad (2.3)$$

where rows denote flavor and columns denote color, with the fourth color being dubbed "lilac" for lepton. The flavor (color) 15-fold gauge bosons  $W_L$  ( $V_L$ ) couple to  $F_L$   $F_L$ , with the W's containing the usual weak and electromagnetic gauge bosons and the V's containing the octet of color gluons:

$$V_{L,R} = \begin{bmatrix} & & & \bar{X}_1 \\ & & & \bar{X}_2 \\ & & & \bar{X}_3 \\ X_1 & X_2 & X_3 & \sqrt{\frac{3}{4}} S^0 \end{bmatrix}_{L,R}, \quad (2.4)$$

The couplings of  $V_{L,R}$  to the fermions is given by

$$\mathcal{L}_{\text{gluon}} = \sum_{\text{flavors}} g_G (\bar{q}_r \bar{q}_y \bar{q}_b)_L \gamma_\mu \frac{\vec{\lambda}}{2} \begin{pmatrix} q_r \\ q_y \\ q_b \end{pmatrix}_L \vec{V}_{L\mu}(\underline{8}) + L + R \quad (2.5a)$$

$$\mathcal{L}_X = \sum_{i=r,y,b} \sum_{\text{flavors}} g_G(\bar{q}_i \gamma_\mu \ell)_L X_{L\mu}^i + L \rightarrow R + \text{h.c.} \quad (2.5b)$$

$$\mathcal{L}_{S^0} = \sum_{\text{flavors}} - \left( \frac{g_G}{2\sqrt{6}} \right) \left( \sum_{i=r,y,b} \bar{q}_i \gamma_\mu q_i - 3\bar{\ell} \gamma_\mu \ell \right)_L S_{L\mu}^0 + L \rightarrow R \quad , \quad (2.5c)$$

where  $q$  denotes quark fields,  $\ell$  denotes leptons, and  $\vec{\lambda}$  are the SU(3) matrices. As in the SU(5) scheme, we see here the possibility for proton decay through the couplings of  $X^i$  to  $\bar{q}\ell$ .

The next important feature is the spontaneous breakdown of the flavor and color symmetries. We begin with the breakdown of the color symmetry. Parity conservation in the strong interactions implies that  $SU(4)_L^C \otimes SU(4)_R^C$  breaks so as to conserve left-right symmetry in the 3-color sector. Also, the mass of the X-particles can be given a lower bound since they induce the unobserved transition  $K_L \rightarrow \bar{\mu}e$  through their couplings to  $(\bar{n}e)$  and  $(\bar{\lambda}\mu)$ . From the experimental upper limit for this process, one gets

$$M_X \gtrsim 10^4 \text{ GeV} \quad . \quad (2.6)$$

In breaking the  $SU(4)_L^C \otimes SU(4)_R^C$  color symmetry, there are two interesting possibilities:<sup>7,15,18</sup>

$$(i) \quad SU(4)_L^C \otimes SU(4)_R^C \xrightarrow{M_I \gg 10^4 \text{ GeV}} SU(4)_{L+R}^C \xrightarrow{M_{II} \gtrsim 10^4 \text{ GeV}} SU(3)^C \otimes \begin{cases} U(1)_{L+R} \text{ or} \\ U(1)_L \otimes U(1)_R \end{cases} \quad (2.7a)$$

$$\begin{array}{ccc}
 \text{(ii) } SU(4)_L^C \otimes SU(4)_R^C & \xrightarrow{M_I \gtrsim 10^4 \text{ GeV}} & SU(3)_L^C \otimes SU(3)_R^C \left\{ \begin{array}{l} U(1)_{L+R} \\ U(1)_L \otimes U(1)_R \end{array} \right. \\
 & & \downarrow \\
 & & SU(3)_{L+R}^C \quad \text{Light Mass } M_{II} \approx \text{few GeV}
 \end{array} \quad (2.7b)$$

In both cases one generates both vector and axial vector color gluons. But in case (ii) the axial vector gluons are low in mass whereas in case (i) they are superheavy. The  $U(1)_{L(R)}$  correspond to the 15th generators of  $SU(4)_{L(R)}^C$  and the gauge particles  $S_{L(R)}^O$  with  $U_{L+R}^C(1)$  being their diagonal sum. In both cases (i) and (ii) the X gauge particles are superheavy with masses probably much larger but at least bounded by Eq. (2.6).

If low mass axial vector gluons are found, they would supplement the standard vector QCD, possibly affecting hyperfine splittings in charmonium spectroscopy. Also, their existence and the resulting larger low energy residual color symmetry as compared to the more standard case (i) would lead to a stronger growth in the color coupling constant relative to the flavor coupling constant for decreasing momentum, thus lowering the unification mass from the usual  $10^{15}$  GeV to  $10^5$  GeV.<sup>18</sup>

The flavor symmetry breaking would proceed as follows:

$$SU(4)_L \otimes SU(4)_R \xrightarrow{M_I \gtrsim 10^4 \text{ GeV}} SU(2)_L \otimes SU(2)_R \xrightarrow{M_{II} \sim M_{W_{R^+}}} SU(2)_L \otimes U(1)_R, \quad (2.8)$$

where electron polarization in  $\beta$  decay gives  $M_{W_{R^+}} \gtrsim 300$  GeV.<sup>15</sup> Combining the surviving symmetry here with the surviving color-singlet piece  $U(1)_L \otimes U(1)_R$  or  $U(1)_{L+R}$  we get

$$G_{\text{flavor}} = SU(2)_L \otimes U(1)_R \otimes \left\{ \begin{array}{l} U(1)_L \otimes U(1)_R \\ \text{or } U(1)_{L+R} \end{array} \right. \quad (2.9)$$

Subsequent symmetry breaking proceeds via a mass-scale  $\lesssim M_{W_L}$  using the Higgs fundamental sets B and C which transform under  $[SU(4)_L \otimes SU(4)_R]^{color} \otimes [SU(4)_L \otimes SU(4)_R]^{flavor}$  as  $B = (1, \bar{4}, 1, 4)$  and  $C = (\bar{4}, 1, 4, 1)$  and having vacuum expectation values

$$\langle B \rangle = \begin{bmatrix} 0 & 0 & 0 & 0 \\ 0 & 0 & 0 & 0 \\ 0 & 0 & 0 & 0 \\ 0 & 0 & 0 & b_4 \end{bmatrix} \quad (2.10a)$$

$$\langle C \rangle = \begin{bmatrix} c_1 & 0 & 0 & 0 \\ 0 & c_1 & 0 & 0 \\ 0 & 0 & c_1 & 0 \\ 0 & 0 & 0 & c_4 \end{bmatrix}, \quad (2.10b)$$

with  $c_1 = 0$  or few GeV. The final level of symmetry breaking proceeds as follows:

$$G_{flavor} = SU(2)_L \otimes U(1)_R \otimes U(1)_{L+R} \begin{matrix} \downarrow \langle B \rangle \\ SU(2)_L \otimes U(1) \\ \downarrow \langle C \rangle \\ U(1)^{EM} \end{matrix} \quad (2.11)$$

While  $b_4$  and  $c_4$  give mass to the weak gauge particles,  $c_1$  provides a mechanism of giving mass to the octet of color gluons, since  $\langle C \rangle$  breaks color as well as flavor. Thus, whether or not there exists an octet of light axial gluons, the low energy three-color symmetry has two interesting possibilities:

(i)  $c_1 = 0$  yields the standard QCD theory with massless neutral vector color gluons and fractionally charged (possibly permanently confined) quarks inside the physical hadrons;

(ii)  $c_1 \sim \text{few GeV}$  leads to both charged and neutral vector color gluons of a few GeV in mass and integrally charged and unconfined quarks inside the physical hadrons.

It is the second possibility on which we will primarily focus in the later sections. In this case there are four neutral and four charged color gluons, all of which acquire the same mass  $\mu_G$ , and an effective global  $SU(3)^C$  symmetry survives, serving as a good classification symmetry.

The  $SU(4)^C$  gauge fields are

$$V = \begin{bmatrix} V_{11} & V_{\rho}^{-} & V_{K^*}^{-} & \bar{X}^0 \\ V_{\rho}^{+} & V_{22} & \bar{V}_{K^*}^0 & X^+ \\ V_{K^*}^{+} & V_{K^*}^0 & V_{33} & X'^+ \\ X^0 & X^{-} & X'^- & \sqrt{\frac{3}{4}} S^0 \end{bmatrix}, \quad (2.12)$$

where

$$V_{11} = \frac{1}{\sqrt{2}} \left( V_3 + \frac{1}{\sqrt{3}} V_8 - \frac{1}{\sqrt{6}} S^0 \right) \quad (2.13a)$$

$$V_{22} = \frac{1}{\sqrt{2}} \left( -V_3 + \frac{1}{\sqrt{3}} V_8 - \frac{1}{\sqrt{6}} S^0 \right) \quad (2.13b)$$

$$V_{33} = \frac{1}{\sqrt{2}} \left( -\frac{2}{\sqrt{3}} V_8 - \frac{1}{\sqrt{6}} S^0 \right), \quad (2.13c)$$

with  $V_{i=1,2,\dots,8}$  being the canonical octet of gluon fields.

Further, since the Higgs B and C carry both flavor and color, the spontaneous symmetry breaking leads to a mixing of the color and flavor gauge particles.<sup>19</sup> For example, the massless photon A has the usual flavor piece  $W^0$  plus some color  $U^0$  mixed in where

$$U^0 = \frac{1}{2}(\sqrt{3} V_3 + V_8) \quad . \quad (2.14)$$

Similarly, there is a gluon  $\tilde{U}$  of mass  $m_{\tilde{U}} \sim g_s c_1 \sim \text{few GeV}$  which is the orthogonal combination of  $W^0$  and  $U^0$ . So, we have

$$A = \cos \delta W^0 + \sin \delta U^0 \quad (2.15a)$$

$$U = -\sin \delta W^0 + \cos \delta U^0 \quad , \quad (2.15b)$$

where

$$\tan \delta \sim \frac{g_f}{g_s} \ll 1 \quad , \quad (2.16)$$

and the coupling constant subscripts refer to flavor (f) and strong (s). The mixing of the charged flavor and color gauge particles is negligible with mass dependent mixing angles  $\sim (m_{V^\pm}/m_{W^\pm})^2 g_f/g_s \ll \ll 1$ .

The fermion electric charges in the Pati-Salam theory can be obtained by first defining flavor and color pieces:

$$Q_{\text{flav}} \equiv (F_3 + \frac{1}{\sqrt{3}}F_8 - \sqrt{\frac{2}{3}}F_{15}) - \sqrt{\frac{2}{3}}F_{15}^C \quad (2.17a)$$

$$Q_{\text{col}} \equiv F_3^C + \frac{1}{\sqrt{3}}F_8^C \quad , \quad (2.17b)$$

where  $F_i$  ( $F_i^C$ ) are the generators of  $SU(4)$  ( $SU(4)^C$ ). Then, the fermion charges are given by

$$Q = Q_{\text{flav}} \quad (\text{fractional charges}) \quad (2.18a)$$

$$Q = Q_{\text{flav}} + Q_{\text{col}} \quad (\text{integral charges}) \quad , \quad (2.18b)$$

where the fractional charge case corresponds to  $c_1 = 0$  and the integral charge case corresponds to  $c_1 \neq 0$ . Hence, the charges corresponding to the fermion matrix  $F$  given in Eq. (2.3) are as follows:

$$\begin{array}{c} \begin{array}{c} \text{Fractional} \\ \left[ \begin{array}{cccc} \frac{2}{3} & \frac{2}{3} & \frac{2}{3} & 0 \\ \frac{1}{3} & \frac{1}{3} & \frac{1}{3} & -1 \\ -\frac{1}{3} & -\frac{1}{3} & -\frac{1}{3} & -1 \\ -\frac{1}{3} & -\frac{1}{3} & -\frac{1}{3} & -1 \\ \frac{2}{3} & \frac{2}{3} & \frac{2}{3} & 0 \end{array} \right] \end{array} \\ \begin{array}{c} \text{Integral} \\ \left[ \begin{array}{cccc} 0 & +1 & +1 & 0 \\ -1 & 0 & 0 & -1 \\ -1 & 0 & 0 & -1 \\ 0 & +1 & +1 & 0 \end{array} \right] \end{array} \end{array} \quad (2.19)$$

Note that  $Q_{\text{col}}(\text{leptons}) = 0$  so that the lepton charges are the same in both cases.

Without being too laborious, we hope that we have touched upon the main features of the Pati-Salam theory necessary for the following discussion of deep-inelastic scattering. In the next section, we present only the lowest order content of the Pati-Salam theory for this process.

### III. DEEP-INELASTIC SCATTERING WITH MASSIVE GLUONS

As opposed to the standard massless QCD model, the massive gluon QCD model contained in the Pati-Salam theory allows the possibility of color production.<sup>19</sup> If we denote color nonsinglet states by  $X_{\text{col}}$  and color singlet flavor states by  $X_{\text{flav}}$ , then the total inclusive amplitude  $A(\ell N \rightarrow \ell + X)$  contains contributions from both  $A(\ell N \rightarrow \ell + X_{\text{flav}})$  and  $A(\ell N \rightarrow \ell + X_{\text{col}})$ . Of course, the latter contributes only if the outgoing state's energy is above some threshold for producing color nonsinglet hadronic states. In that case, the order  $e^2$  diagrams for  $A(\ell N \rightarrow \ell + X_{\text{col}})$  would be as shown in Fig. 1. Thus, one calculates

$$\begin{aligned} A(\ell N \rightarrow \ell + X_{\text{col}}) &= e^2 \bar{\ell} \gamma_\mu \ell \left( \frac{1}{q^2} - \frac{1}{q^2 - m_{\tilde{U}}^2} \right) \langle X_{\text{col}} | J_{\text{col}}^\mu | N \rangle \\ &= e^2 \frac{\bar{\ell} \gamma_\mu \ell}{q^2} \left( \frac{-m_{\tilde{U}}^2}{q^2 - m_{\tilde{U}}^2} \right) \langle X_{\text{col}} | J_{\text{col}}^\mu | N \rangle \quad , \quad (3.1) \end{aligned}$$

where we can define the damping factor

$$\Delta \equiv \frac{-m_{\tilde{U}}^2}{q^2 - m_{\tilde{U}}^2} \quad . \quad (3.2)$$

For the amplitude  $A(\ell N \rightarrow \ell + X_{\text{flav}})$ , only the first diagram in Fig. 1 contributes with  $X_{\text{col}}$  replaced by  $X_{\text{flav}}$  and we get

$$A(\ell N \rightarrow \ell + X_{\text{flav}}) = \frac{e^2 \bar{\ell} \gamma_\mu \ell}{q^2} \langle X_{\text{flav}} | J_{\text{flav}}^\mu | N \rangle \quad , \quad (3.3)$$

where

$$J_{\text{flav}}^{\mu} = \left( \sum_{\alpha=\text{red,yellow,blue}} \frac{2}{3} \bar{p}_{\alpha} \gamma^{\mu} p_{\alpha} - \frac{1}{3} \bar{n}_{\alpha} \gamma^{\mu} n_{\alpha} - \frac{1}{3} \bar{\lambda}_{\alpha} \gamma^{\mu} \lambda_{\alpha} + \frac{2}{3} \bar{c}_{\alpha} \gamma^{\mu} c_{\alpha} \right) - (\bar{e} \gamma^{\mu} e + \bar{\mu} \gamma^{\mu} \mu) \quad (3.4a)$$

$$J_{\text{col}}^{\mu} = \sum_{q=p,n,\lambda,c} -\frac{2}{3} \bar{q}_{\text{red}} \gamma^{\mu} q_{\text{red}} + \frac{1}{3} \bar{q}_{\text{yellow}} \gamma^{\mu} q_{\text{yellow}} + \frac{1}{3} \bar{q}_{\text{blue}} \gamma^{\mu} q_{\text{blue}} \quad (3.4b)$$

Below the threshold for color production, only the photon  $\gamma$  contributes and it sees only the fractional flavor charges of the quark partons. Hence, there is no observable difference between the  $c_1 = 0$  and  $c_1 \neq 0$  alternatives (see Section II). However, above the color threshold, both  $\gamma$  and  $\tilde{U}$  contribute, quark partons interact through their flavor plus color integral charges, and the charged members of the color gluon octet ( $V_{\rho}^{\pm}, V_{K^*}^{\pm}$ ) become active partons. The  $c_1 = 0$  possibility does not permit a color threshold, and thus the experimental verification of the existence of such a threshold would place the standard massless gluon QCD model in jeopardy.

In the following we focus on the  $c_1 \neq 0$  case and write the structure functions as follows:<sup>20</sup>

$$F_i = F_i^{\text{flav}} + F_i^{\text{col}} \theta(W - M_{\text{col}}) \quad , \quad (3.5)$$

with

$$W = M_N^2 + \left( \frac{1-x}{x} \right) Q^2 \quad (3.6)$$

and where  $Q^2$  is the squared momentum of the probe,  $M_{\text{col}}$  is the invariant mass of the lightest color octet hadronic final state,  $F_i^{\text{flav}}$  is the standard fractionally

charged quark model result, and  $F_i^{\text{col}}$  is to be calculated from the diagrams shown in Fig. 2. In evaluating the diagrams, one uses the massive gluon spin sum  $-g_{\mu\nu} + p_\mu p_\nu / \mu_G^2$ , where the gluon mass  $\mu_G \ll$  nucleon mass  $M_N$  inside the nucleonic environment. Outside the nucleon, however, the gluon mass would perhaps be several GeV as discussed in Section II. The result for  $F_i^{\text{col}}$  is

$$F_1^{\text{col}} = \left[ \bar{m}_{\tilde{U}}^2 / (Q^2 + \bar{m}_{\tilde{U}}^2) \right]^2 \left\{ \frac{1}{9} \sum_{q_i} [q_i(x) + \bar{q}_i(x)] + \frac{16}{3} \left( 1 + \frac{Q^2}{4\bar{\mu}_G^2} \right) v(x) \right\} \rho_{\text{col}}^{\text{Th}}(Q^2, W^2) \quad (3.7a)$$

$$F_2^{\text{col}} = \left[ \bar{m}_{\tilde{U}}^2 / (Q^2 + \bar{m}_{\tilde{U}}^2) \right]^2 \left\{ \frac{2}{9} \sum_{q_i} [q_i(x) + \bar{q}_i(x)] + \left( 4 + \frac{4}{3} \frac{Q^2}{\bar{\mu}_G^2} + \frac{1}{3} \frac{Q^4}{\bar{\mu}_G^4} \right) v(x) \right\} x \rho_{\text{col}}^{\text{Th}}(Q^2, W^2) \quad (3.7b)$$

where  $q_i(x)$  is the momentum distribution function for the  $i$ th quark flavor,  $v(x)$  is the momentum distribution function for any one of the gluon partons, as usual  $x = Q^2/2M_N v$ , and  $\rho_{\text{col}}^{\text{Th}}$  is the scale-threshold factor signifying that scaling (up to log corrections) is not realized until  $W$  is several GeV above  $M_{\text{col}}$ . In Section VII, we shall use the form employed in Ref. 20:

$$\rho_{\text{col}}^{\text{Th}}(Q^2, W) \Big|_{Q^2 > 1 \text{ GeV}^2} = \theta(W - M_{\text{col}}) (1 - (M_{\text{col}}/W)^2)^\alpha \quad (3.8)$$

We shall choose the exponent  $\alpha$  so that  $\rho_{\text{col}}^{\text{Th}}$  acquires a 75% saturation as  $W$  increases from  $M_{\text{col}}$  to  $M_{\text{col}} + 2 \text{ GeV}$ .

Equations (3.7a-b) can be greatly simplified. First note that precocious scaling at SLAC for  $Q^2 \gtrsim 1 \text{ GeV}^2$  seems to imply that quark and gluon parton

masses are much less than 1 GeV at  $Q^2 = 1 \text{ GeV}^2$ , so that  $\bar{\mu}_G(Q^2 = 1 \text{ GeV}^2) \lesssim 100\text{--}300 \text{ MeV} \ll 1 \text{ GeV}$ . So, we expect  $Q^2/\bar{\mu}_G^2$  to exceed 10 and perhaps even 100 at  $Q^2 = 1 \text{ GeV}^2$  and to grow even larger as  $Q^2$  increases. Next, note that not only must the gluon propagator mass  $\bar{m}_{\tilde{U}}$  be evaluated at  $q^2$ , but in the operator product expansion for the standard hadronic tensor  $W_{\mu\nu}(p, q)$ , the gluon parton mass  $\bar{\mu}_G$  must also be evaluated at  $q^2$ .<sup>20</sup> Hence, we can set  $\bar{m}_{\tilde{U}} = \bar{\mu}_G$  for our purposes. The result is that for  $Q^2 \gtrsim 1\text{--}2 \text{ GeV}^2$ , Eqs. (3.7a-b) reduce to the following simple expressions for the nucleon color structure functions:

$$F_1^{\text{col}} \approx 0 \quad (3.9a)$$

$$F_2^{\text{col}} \approx \frac{1}{3} x v(x) \rho_{\text{col}}^{\text{Th}}(Q^2, W^2) \quad (3.9b)$$

Note that the main contribution to  $F_2^{\text{col}}$  comes from the gluon partons and not from quark or scalar partons. And since the gluons reside at  $x \lesssim 0.3$ , one would expect color production to be a characteristically low  $x$  phenomenon. Also, note in Eq. (3.9b) that, aside from the factor  $\rho_{\text{col}}^{\text{Th}}$  which has little effect anyway, scaling (up to log corrections) is retrieved. Had it not been for the damping factor  $\Delta^2$  in Eqs. (3.7a-b) this would not have been so, and  $F_i^{\text{col}}$  would have had a bad high  $Q^2$  behavior. Thus we see the utility of the gauge approach to integrally charged quarks and spin-1 gluon partons.

Now that we have the lowest order formulae for the nucleon color structure functions in terms of parton distributions, in the next section we begin a discussion of the Altarelli-Parisi method for calculating the higher order corrections.

#### IV. ALTARELLI-PARISI PARTON TRANSITION FUNCTIONS WITH MASSIVE GLUONS

The Altarelli-Parisi program<sup>13</sup> for calculating higher order  $Q^2$ -dependent corrections to parton distribution functions is well known in the case of massless gluons. The evolution in  $Q^2$  is obtained by solving the following equations:

$$\frac{dq_{NS}(x, t)}{dt} = \frac{\alpha(Q^2)}{2\pi} \int_x^1 \frac{dy}{y} q_{NS}(y, t) P_{qq}\left(\frac{x}{y}\right) \quad (4.1a)$$

$$\frac{dq_S(x, t)}{dt} = \frac{\alpha(Q^2)}{2\pi} \int_x^1 \frac{dy}{y} \left[ q_S(y, t) P_{qq}\left(\frac{x}{y}\right) + 2fG(y, t) P_{qG}\left(\frac{x}{y}\right) \right] \quad (4.1b)$$

$$\frac{dG(x, t)}{dt} = \frac{\alpha(Q^2)}{2\pi} \int_x^1 \frac{dy}{y} \left[ q_S(y, t) P_{Gq}\left(\frac{x}{y}\right) + G(y, t) P_{GG}\left(\frac{x}{y}\right) \right], \quad (4.1c)$$

where  $f$  is the number of quark flavors and

$$q_{NS} = q_i(x) - q_j(x), \text{ etc.} \quad (4.2a)$$

$$q_S = \sum_i q_i(x) + \bar{q}_i(x) \quad (4.2b)$$

$$\alpha(Q^2) = \frac{g^2(Q^2)}{4\pi} \quad (4.2c)$$

$$t = \ln \frac{Q^2}{\mu^2}, \quad (4.2d)$$

with  $q_{NS}$  and  $q_S$  denoting flavor nonsinglet and singlet quark distributions, respectively,  $i$  and  $j$  denoting quark flavors, and  $\mu$  being the renormalization point of the theory.

We refer to the  $P_{BA}(z)$  as the parton transition functions. In the standard massless gluon QCD theory, they can be derived from the elementary QCD vertices alone. As such,  $\alpha/2\pi P_{BA}(z)$  can readily be interpreted as the probability density per unit  $t$  of finding inside parton A a parton B with fraction  $z$  of A's momentum. In order to obtain  $P_{BA}(z)$  from the elementary vertices alone one uses a noncovariant polarization sum over only transverse gluons and neglect diagrams wherein partons are emitted after the probe scatters off of the initial parton. However, this procedure is not well suited for the massive gluon Pati-Salam model, since gluons in this case have longitudinal in addition to transverse components. Ellis et al.<sup>21</sup> have discussed the Altarelli-Parisi program in an entirely covariant framework, and it is their approach which we discuss in the case of massive gluons.<sup>22</sup>

To illustrate the procedure using massless gluons, we show the diagrams for calculating  $P_{qq}$  in Fig. 3. In the massless gluon theory the probe is the photon  $\gamma$ . One calculates the differential scattering cross-section to order  $\alpha$  in the strong coupling constant for scattering  $\gamma$  off of the quark parton of  $i$ th flavor carrying momentum  $p_1$ . For simplicity consider only the cross-section which is projected out by contracting the indices of the probe with  $(-g_{\mu\nu})$ . In terms of the parton "scaling variable"

$$z = \frac{Q^2}{2p_1 \cdot q} \quad (4.3)$$

one gets<sup>21</sup>

$$\frac{d\sigma_i}{dz} = e_i^2 \left\{ \delta(1-z) + \frac{\alpha}{2\pi} \frac{4}{3} \left[ \frac{1+z^2}{(1-z)_+} + \frac{3}{2} \delta(1-z) \right] \ln \left( \frac{q^2}{p_1^2} \right) \right\} \quad , \quad (4.4)$$

where the distribution  $(1 - z)_+^{-1}$  is defined by the following:

$$\int_0^1 dz \frac{h(z)}{(1-z)_+} \equiv \int_0^1 dz \frac{h(z) - h(1)}{(1-z)} \quad , \quad (4.5)$$

with  $h(z)$  being any test function regular at the endpoints.

The function of interest  $P_{qq}$  is the coefficient of the infrared singular factor  $\ln(q^2/p_1^2)$  occurring in Eq. (4.4). Thus, an algorithm for calculating the  $P_{BA}$ 's is simply to extract the coefficients of the infrared singular factors in the appropriate differential scattering cross sections.

For the case of massive gluons, the analogy is that to each order in  $\alpha$  we extract the coefficient of the leading power in  $-q^2/\mu_G^2$ . However, one must keep in mind that diagrams such as are shown in Fig. 3 are only an isolated part of the overall lepton-parton scattering process. Hence, the large  $-q^2$  behavior in the overall process does not present a problem since it is damped by the previously discussed factor  $\Delta^2$  [cf. Eq. (3.2)]. In the massless gluon case discussed above, the infrared singular factors are not damped but are absorbed into the bare parton distribution functions to form finite renormalized parton distribution functions.<sup>21</sup> Note that one must not think that terms of higher order in  $\alpha$  dominate those of lower order in  $\alpha$  as a result of the powers of  $-q^2/\mu_G^2$ . Even for the case of confined QCD one cannot naively look at the  $\ln(q^2/p_1^2)$  factor from the order  $\alpha$  contributions in Fig. 3 to conclude that they are larger than the lowest order parton model result (first diagram of Fig. 3). For each order in  $\alpha$  one must retain the leading  $\ln(q^2/p_1^2)$  contribution. This is analogous to what we do in the Pati-Salam theory. To find corrections to the lowest order probe-parton scattering, we calculate the order  $\alpha$  diagrams and retain the terms of leading order in  $-q^2/\mu_G^2$ . A comparison of parton model diagrams to the appropriate ones in the operator product formalism makes the above immediately clear.

We can now calculate  $P_{qq}(z)$  in the massive gluon theory above the color threshold where the probe sees the color charges of the partons. The relevant diagrams are the same as in the massless gluon case and are shown in Fig. 3. Using the above algorithm, we calculate the cross section  $d\sigma_{qq}/dz$  for scattering the probe  $U^0$ --the color piece of both the photon and its orthogonal partner  $\tilde{U}$ --off the initial parton to order  $\alpha$ . Since the red, yellow, blue quark color electric charges are  $-2/3, 1/3, 1/3$ , respectively, we take  $-ie\gamma_\mu (2 \cdot 3^{-1/2} t^0)$  as our  $U^0 q\bar{q}$  vertex, where

$$t^0 = \frac{1}{2}(\sqrt{3}t^3 + t^8) \quad (4.6a)$$

obeying

$$[t^0, t^j] = if_{0jk}t^k \quad (4.6b)$$

$$\text{Tr}(t^0 t^0) = \frac{1}{2} \quad , \quad (4.6c)$$

with

$$f_{0jk} \equiv \frac{1}{2}(\sqrt{3}f_{3jk} + f_{8jk}) \quad (4.6d)$$

and  $t^i$  being the usual  $SU(3)$  matrices. For the gluon partons (G), the  $U^0 G^a G^b$  vertex carries the color factor  $f^{cab}$ .

All relevant phase space factors are contained in ref. 21. We define

$$y = p_1 \cdot p_2 / p_1 \cdot q \quad , \quad (4.7)$$

where  $p_{1,2}$  are the parton momenta as indicated in the figures. First express all amplitudes in terms of the usual  $s, t, u, q^2, p_1^2$  dropping terms  $O(p_2^2, p_3^2)$ . They are then expressed in terms of  $p_1^2, q^2, y, z$  using Eqs. (4.3) and (4.7) and the following:

$$s = p_1^2 + 2p_1 \cdot q(1 - z) \quad (4.8a)$$

$$t = -2p_1 \cdot q(1 - y) \quad (4.8b)$$

$$u = p_1^2 - 2yp_1 \cdot q \quad (4.8c)$$

Finally, we neglect all terms of  $O(p_1^2)$ , being careful to retain only the leading terms in  $q^2/p_1^2$ , and perform the  $y$  integration from 0 to  $y \approx 1 - p_1^2/q^2$  (see ref. 21).

After performing the appropriate average (sum) over initial (final) spin and color for the diagrams in Fig. 3, we obtain

$$|\bar{M}_{qq}|^2 = \frac{1}{3} e^2 g^2 \frac{q^2}{\mu_G^2} \left( \frac{s}{q^2} + \frac{t}{q^2} - 1 \right) \quad (4.9)$$

yielding

$$\frac{d\sigma_{qq}}{dz} = \frac{e^2 \alpha}{2\pi} \frac{-q^2}{\mu_G^2} \frac{1}{6} \frac{1}{z} \quad (4.10)$$

Thus,

$$P_{qq}(z) = \frac{1}{6z} \quad (4.11)$$

We show the parton diagrams for calculating  $P_{Gq}(z)$ ,  $P_{qG}(z)$ , and  $P_{GG}(z)$  in Figs. 4, 5, and 6, respectively. The calculations are as outlined above and are quite laborious. The results are

$$P_{Gq}(z) = \frac{1-z}{6} \quad (4.12a)$$

$$P_{qG}(z) = \frac{1}{24} \frac{z^3 - 5z^2 + \frac{31}{4}z - \frac{11}{3}}{z(1-z)^2} \quad (4.12b)$$

$$P_{GG}(z) = \frac{1}{32} \left( \frac{3}{2} \frac{1}{z^3} - \frac{1}{z^2} - 1 \right) \quad (4.12c)$$

The Higgs sector of the theory can be neglected as has been discussed previously.<sup>22,23</sup> Also, all the results have been checked to be gauge invariant. We find that the  $P_{BA}$ 's do not obey the same set of symmetry relations as for the massless case. This is because the results cannot be derived from the elementary QCD vertices alone as was done in Ref. 13. Perhaps they can no longer simply be interpreted as probability densities.

Before going ahead with the results of this section and calculating higher order corrections to parton distributions above the color production threshold, in the next section we first discuss the phenomenology of parton distributions below the color threshold.

### V. PARTON DISTRIBUTIONS BELOW THE COLOR THRESHOLD

Before discussing the solutions to the Altarelli-Parisi Eqs. (4.1) above the color threshold, we first discuss their solutions in the absence of color production. This would correspond to the  $F_i^{\text{flav}}$  discussed in Sec. III [cf. Eq. (3.5)]. For the valence quarks, we use the parametrizations of Buras and Gaemers.<sup>24</sup> Define  $u \equiv u_v + \xi$ ,  $d = d_v + \xi$ , and  $\bar{u} \approx \bar{d} \approx s \approx \bar{s} \equiv \xi$ , where the subscripts denote valence quark distributions and  $\xi$  denotes the sea. The Buras-Gaemers valence quark distributions are as follows:

$$xu_v(x, Q^2) + xd_v(x, Q^2) = \frac{3}{B(\eta_1, 1 + \eta_2)} x^{\eta_1} (1-x)^{\eta_2} \quad (5.1a)$$

$$xd_v(x, Q^2) = \frac{1}{B(\eta_3, 1 + \eta_4)} x^{\eta_3} (1-x)^{\eta_4} \quad (5.1b)$$

with

$$\eta_1 = 0.70 - 0.176s \quad (5.2a)$$

$$\eta_2 = 2.60 + 0.80s \quad (5.2b)$$

$$\eta_3 = 0.85 - 0.24s \quad (5.2c)$$

$$\eta_4 = 3.35 + 0.816s \quad , \quad (5.2d)$$

where

$$s = \ln \left[ \frac{\ln(Q^2/\Lambda^2)}{\ln(Q_0^2/\Lambda^2)} \right] \quad , \quad (5.3)$$

$Q_0^2 = 1.8 \text{ GeV}^2$ ,  $\Lambda = 0.5 \text{ GeV}$ , and  $B(\eta_i, 1 + \eta_{i+1})$  is the Euler beta function which insures baryon number conservation for all values of  $Q^2$ .

For the sea quarks and gluons, we use the parametrizations of Owens and Reya<sup>14</sup> and add in the contributions from the charmed sea. The Owens-Reya sea and gluon distributions are written as follows:

$$x\xi(x, Q^2) = A_s(1-x)^{\eta_s} + A'_s(1-x)^{\eta'_s} + B_s e^{-C_s x} \quad (5.4a)$$

$$xG(x, Q^2) = A_g(1-x)^{\eta_g} + A'_g(1-x)^{\eta'_g} + B_g e^{-C_g x} \quad , \quad (5.4b)$$

where the coefficients and exponents are written as the following polynomials in  $s$ :

$$A_i = A_i^{(0)} + A_i^{(1)}s + A_i^{(2)}s^2 \quad (5.5a)$$

$$\eta_i = \eta_i^{(0)} + \eta_i^{(1)}s + \eta_i^{(2)}s^2 \quad (5.5b)$$

$$A'_i = A'_i^{(1)}s + A'_i^{(2)}s^2 \quad (5.5c)$$

$$\eta'_i = \eta'_i^{(0)} + \eta'_i^{(1)}s + \eta'_i^{(2)}s^2 \quad (5.5d)$$

$$B_i = B_i^{(1)}s + B_i^{(2)}s^2 \quad (5.5e)$$

$$C_i = C_i^{(0)} + C_i^{(1)}s + C_i^{(2)}s^2 \quad , \quad (5.5f)$$

with these coefficients being displayed in Table I. The above parametrizations should be valid over the region  $0.02 \leq x \leq 0.8$ .

Using the above parametrizations, typically about 6% of the parent nucleon's momentum is unaccounted for for  $Q^2$  up to  $\sim 100 \text{ GeV}^2$ . We can reduce this to 1 to 2% by including the Buras-Gaemers charmed sea  $C \equiv c + \bar{c} = 2c$ :<sup>24</sup>

$$xC(x, Q^2) = \langle C(Q^2) \rangle_2 \left[ \frac{\langle C(Q^2) \rangle_2}{\langle C(Q^2) \rangle_3} - 1 \right] (1-x) \left[ \frac{\langle C(Q^2) \rangle_2}{\langle C(Q^2) \rangle_3} - 2 \right], \quad (5.6)$$

where

$$\langle C(Q^2) \rangle_n \equiv \int_0^1 dx x^{n-1} C(x, Q^2), \quad n \geq 2 \quad (5.7)$$

is the charmed quark's  $n$ th moment which we calculate using the Owens-Reya strange quark distribution and the well-known QCD formula<sup>25</sup>

$$\langle c(Q^2) \rangle_n - \langle s(Q^2) \rangle_n = \left[ \langle c(Q_0^2) \rangle_n - \langle s(Q_0^2) \rangle_n \right] \exp \left[ -d_{NS}^n \right], \quad (5.8)$$

with  $d_{NS}^n$  being proportional to the anomalous dimension of the spin  $n$  nonsinglet operator as defined in Ref. 12 and first calculated in Refs. 1 and 2. We take  $\langle c(Q_0^2) \rangle_n = 0$ .

We plot in Figs. 7(a-f) the proton structure function  $F_2^{p, \text{flav}}(x, Q^2)$  calculated using the above parton distribution functions for  $x = 0.05882, 0.10, 0.22222, 0.28571, 0.40, \text{ and } 0.66667$ , respectively. The data points are taken from Gordon et al.<sup>26</sup> For comparison, we display  $F_2^{p, \text{flav}}(x, Q^2)$  calculated from the Owens-Reya distributions taking  $c(x, Q^2) = 0$ . Gordon et al. fit their full  $F_2^{p, \text{flav}}$  data over the ranges  $0 \lesssim x \lesssim 0.7$  and  $1 \text{ GeV}^2 \lesssim Q^2 \lesssim 65 \text{ GeV}^2$  with the following phenomenological formula which we also show in Figs. 7(a-f):

$$F_2^{D,flav}(x, Q^2) = \left[ \sum_{i=1}^3 a_i (1-x)^i \right] \left( \frac{Q^2}{Q_0^2} \right)^{c_1 + c_2 \ln(1-x)}, \quad (5.9)$$

where

$$Q_0^2 = 3 \text{ GeV}^2 \quad (5.10a)$$

$$a_1 = 0.0126 \pm 0.0147 \quad (5.10b)$$

$$a_2 = 0.9986 \pm 0.0394 \quad (5.10c)$$

$$a_3 = -0.6225 \pm 0.0278 \quad (5.10d)$$

$$c_1 = 0.1577 \pm 0.0095 \quad (5.10e)$$

$$c_2 = 0.5329 \pm 0.0195 \quad (5.10f)$$

In general, we find that the Owens-Reya parton distributions with charm added in the manner we described above gives better agreement with both the data points of Gordon et al. and their phenomenological formula than the Owens-Reya distributions without charm. Moreover, the difference between the proton flavor structure functions as calculated from Owens-Reya with charm and from the phenomenological formula of Gordon et al. is typically less than the experimental errors in the data.

Now that we have parton distributions which describe  $F_2^{flav}$  well, in the next section we proceed to calculate the QCD corrections to  $F_2^{col}$ .

## VI. HIGHER ORDER CORRECTIONS TO THE NUCLEON COLOR STRUCTURE FUNCTION

So far, we have just concerned ourselves with parton distributions necessary to describe  $F_2^{\text{flav}}$ . To include the possibility of color production, we need the leading order QCD correction to Eq. (3.9b); therefore, we must solve the Altarelli-Parisi evolution equations [cf. Eqs. (4.1a-c)] for  $G(x, Q^2) = 8v(x, Q^2)$  both below and above the color threshold  $Q_{\text{Th}}^2$  for fixed  $x$ . Below color threshold,  $G(x, Q^2)$  evolves according to the conventional QCD formalism;<sup>23</sup> however, above color threshold, the evolution of  $G(x, Q^2)$  is governed by the new  $P_{Gq}$  and  $P_{GG}$  calculated in Sec. IV.

To solve these evolution equations, we follow the procedure of Feynman, Fields and Ross<sup>27</sup> and first define

$$A \otimes B \equiv \int_x^1 \frac{dz}{z} A\left(\frac{x}{z}\right)B(z) \quad . \quad (6.1)$$

Then we can write the Altarelli-Parisi evolution equations for the parton distributions above color threshold as follows:

$$\frac{d}{d\kappa} \begin{bmatrix} \Sigma(x, Q^2) \\ G(x, Q^2) \end{bmatrix} = \begin{bmatrix} P_{qq} & 2n_f P_{qG} \\ P_{Gq} & P_{GG} \end{bmatrix} \otimes \begin{bmatrix} \Sigma(z, Q^2) \\ G(z, Q^2) \end{bmatrix} \quad , \quad (6.2)$$

where the  $P_{BA}$  are given in Eqs. (4.11) and (4.12),  $\Sigma$  is the total singlet quark distribution summed over all flavors,  $n_f$  is the number of quark flavors which we take to be four, and

$$\kappa = \frac{2}{(11 - \frac{2}{3}n_f)} \ln \left[ \frac{\ln \left( \frac{Q^2}{\Lambda^2} \right)}{\ln \left( \frac{Q_{Th}^2}{\Lambda^2} \right)} \right] \quad (6.3)$$

Equation (6.2) can be written symbolically as

$$\frac{d}{d\kappa} \mathcal{D}(x, Q^2) = \mathcal{P} \otimes \mathcal{D}(z, Q^2) \quad (6.4)$$

with

$$\mathcal{D}(x, Q^2) \equiv \begin{bmatrix} \Sigma(x, Q^2) \\ G(x, Q^2) \end{bmatrix} \quad (6.5a)$$

$$\mathcal{P}(x, Q^2) \equiv \begin{bmatrix} P_{qq} & 2n_f P_{qG} \\ P_{Gq} & P_{GG} \end{bmatrix} \quad (6.5b)$$

Then the solution to Eq. (6.4) can be written formally as

$$\mathcal{D}(x, Q^2) = \exp(\kappa \mathcal{P} \otimes) \mathcal{D}(Q_{Th}^2) \quad (6.6)$$

We only need the gluon part of the solution since only the gluon distribution  $v(x, Q^2) \equiv 1/8 G(x, Q^2)$  contributes to  $F_2^{col}$  at large  $Q^2$ . One must also keep in mind that Eq. (6.6) is applicable only for  $Q^2 \geq Q_{Th}^2$  and that the boundary condition for Eq. (6.4) is chosen so that  $G(x, Q^2)$  from the gluon evolution below color threshold just matches that from Eq. (6.6) at  $Q^2 = Q_{Th}^2$ .

After expanding Eq. (6.6) in  $\kappa$  and doing the integrals numerically, we find that for our purposes it is sufficient to retain only the leading and order  $\kappa$  terms.

We find that the term of order  $\kappa$  is typically only a few percent of the leading term for  $Q_{Th}^2 \leq Q^2 \leq 100 \text{ GeV}^2$ .

As mentioned in the introduction, to obtain an expression for  $F_2^{col}$  with its QCD corrections, one simply replaces  $v(x)$  in Eq. (3.9b) by the  $v(x, Q^2)$  obtained in this section. Having done this, in the next section we show the effects of color production on the isoscalar nucleon structure function.

## VII. QCD CORRECTED EFFECTS OF COLOR PRODUCTION ON THE NUCLEON STRUCTURE FUNCTION

In this section we study the nucleon isoscalar structure function  $F_2$ , which as we recall from Eq. (3.5) is composed of both flavor  $F_2^{flav}$  and color  $F_2^{col}$  pieces. In Secs. V and VI we discussed the QCD corrections to  $F_2^{flav}$  and  $F_2^{col}$ , respectively. Now, it would be interesting to compare our results with data taken from Ball et al.<sup>3</sup> In Figs. 8(a-e) we plot  $F_2$  per nucleon vs.  $Q^2$  at  $x = 0.11, 0.16, 0.21, 0.26,$  and  $0.33$ , respectively, assuming  $M_{col} = 9 \text{ GeV}$ . Note in particular that for  $x = 0.16$  and  $0.21$  the Pati-Salam theory with our parton parametrizations does not agree with the large increases of  $F_2$  reported by Ball et al. Also note that for  $x \gtrsim 0.26$ , the effects due to color production are quite small and virtually impossible to detect experimentally; thus, one would expect the data to lie along the  $F_2^{flav}$  curve which the data points of Ball et al. do for these  $x$  values. Lehman<sup>4</sup> has discussed the data of Ball et al. from the point of view of color excitation; however, we do not predict as large an increase in  $F_2$  due to color production as does Lehman. It is important to note that the anomalously large data points of Ball et al. have been reanalyzed by Ball<sup>28</sup> and lowered to values more in line with the conventional QCD prediction.

In Figs. 9(a-g) we show the percentage increase in  $F_2$  above the conventional QCD prediction for an isoscalar nucleon target due to color production. We examine the values  $M_{col} = 9, 11, 15, 20 \text{ GeV}$  at  $x = 0.03, 0.04, 0.05, 0.10, 0.15, 0.20,$

0.25. These graphs tell us that due to the relative size of the experimental errors, color production would indeed be a difficult effect to observe for all but the smallest values of  $x$ ; preferably  $x \lesssim 0.05$ .

### VIII. DISCUSSION AND SUMMARY

We have discussed deep-inelastic scattering in detail within the context of the Pati-Salam model which allows for the possibility of producing color nonsinglet hadronic states. Leading order QCD effects were calculated for  $F_2^{\text{flav}}$  and  $F_2^{\text{col}}$ , and the expected percentage increase due to color production in the nucleon isoscalar structure function  $F_2$  was presented. The data points of Ball et al.<sup>3</sup> do not agree with our theoretical predictions assuming  $M_{\text{col}} \approx 9$  GeV. However, it is clear that if one is to observe color production, it is necessary to concentrate on small  $x$  values, preferably  $\lesssim 0.05$ . One problem in trying to observe color production is that, aside from very small values of  $x \lesssim 0.05$ , the increase in  $F_2$  due to color production may be less than the experimental errors and thus may be lost in the noise. Since we cannot predict  $M_{\text{col}}$  theoretically, in Figs. 9(a-g) we showed the percentage increase in  $F_2$  assuming various values of  $M_{\text{col}}$ . In any event, we have worked out the theory sufficiently so that the increase in  $F_2$  due to any value of  $M_{\text{col}}$  can be easily calculated.

We note that the Berkeley-FNAL-Princeton Collaboration and the European Muon Collaboration<sup>6</sup> have not seen the  $F_2$  enhancement of Ball et al. However, a word of caution is that none of the more recent experiments give a complete set of data spanning the region  $1$  to  $2 \text{ GeV}^2 \lesssim Q^2 \lesssim 50 \text{ GeV}^2$  for  $x \lesssim 0.05$  where we predict color production would most noticeably manifest itself. Until this region spanning both low and high  $Q^2$  for small  $x$  is exhausted, we do not believe that color production can be conclusively ruled out.

## ACKNOWLEDGMENTS

We have greatly benefited from stimulating discussions with Professors J. Pati, S. Oneda, A. Skuja, W. Caswell, A. Buras, R. Hartung, and Mr. A. Janah.

## FOOTNOTES AND REFERENCES

- <sup>1</sup> H. Georgi and H. Politzer, Phys. Rev. D9 (1974) 416.
- <sup>2</sup> D. Gross and F. Wilczek, Phys. Rev. D8 (1973) 3633; D9 (1974) 980.
- <sup>3</sup> R. Ball et al., Phys. Rev. Lett. 42 (1979) 866.
- <sup>4</sup> E. Lehman, Phys. Rev. Lett. 42 (1979) 869.
- <sup>5</sup> M. Özer and J. Pati, Nucl. Phys. B159 (1979) 293.
- <sup>6</sup> For a discussion of these experiments, see E. Gabathuler in Proceedings of the International Conference on High-Energy Physics, ed. A. Zichichi (CERN, Geneva, Switzerland, 1979), p. 697.
- <sup>7</sup> J. Pati and A. Salam, Phys. Rev. D8 (1973) 1240; D10 (1974) 275.
- <sup>8</sup> S. Weinberg, Phys. Rev. Lett. 19 (1967) 1264.
- <sup>9</sup> A. Salam, in Elementary Particle Theory, ed. N. Svartholm (Almqvist and Wiksell, Stockholm, 1968).
- <sup>10</sup> H. Georgi and S. Glashow, Phys. Rev. Lett. 32 (1974) 438.
- <sup>11</sup> J. Bjorken, Phys. Rev. 179 (1969) 1547.

- <sup>12</sup>For a good review, see A. Buras, *Rev. of Mod. Phys.* 52 (1980) 199.
- <sup>13</sup>G. Altarelli and G. Parisi, *Nucl. Phys.* B126 (1977) 298.
- <sup>14</sup>J. Owens and E. Reya, *Phys. Rev.* D17 (1978) 3003.
- <sup>15</sup>J. Pati, in Topics in Quantum Field Theory and Gauge Theories, Proceedings of the VIII International Seminar on Theoretical Physics held by GIFT in Salamanca, ed. J. de Azcárraga (Springer-Verlag, New York, 1978).
- <sup>16</sup>J. Pati, in Fundamentals of Quark Models, Proceedings of the 17th Scottish Universities Summer School in Physics, ed. I. Barbour and A. Davies (Scottish Universities Summer School in Physics, St, Andrews, 1976).
- <sup>17</sup>We have simplified the discussion here somewhat. With chiral gauging, triangle anomalies are cancelled by introducing mirror fermions. For a complete discussion of this point, see Ref. 15.
- <sup>18</sup>V. Elias et al., *Phys. Rev. Lett.* 40 (1978) 920.
- <sup>19</sup>J. Pati and A. Salam, *Phys. Rev. Lett.* 36 (1976) 11; G. Rajasekharan and P. Roy, *Pramana* 5 (1975) 303 and *Phys. Rev. Lett.* 36 (1976) 355.
- <sup>20</sup>M. Özer and J. Pati, *Nucl. Phys.* B159 (1979) 293.
- <sup>21</sup>R. Ellis et al., *Nucl. Phys.* B152 (1979) 285; for related discussions see: D. Amati et al., *Nucl. Phys.* B146 (1978) 29; Y. Dokshitzer et al., *Proc. Leningrad Winter School* (1978); C. Llewellyn-Smith, Oxford preprint 47/78.
- <sup>22</sup>S. Mtingwa, *Phys. Lett.* 92B (1980) 171.
- <sup>23</sup>N. Craigie and A. Salam, *Phys. Lett.* 85B (1979) 57.
- <sup>24</sup>A. Buras and K. Gaemers, *Nucl. Phys.* B132 (1978) 249.
- <sup>25</sup>For a discussion of Eq. (5.8) and QCD in general, see Ref. 12.
- <sup>26</sup>B. Gordon et al., *Phys. Rev.* D20 (1979) 2645.

<sup>27</sup>For a discussion of this procedure, see R. Field, Calt-68-739 (1979).

<sup>28</sup>R. Ball, Measurement of the Structure Function  $F_2$  in Muon Scattering at 270 GeV, Ph.D. thesis, Michigan State University, 1979.

	$A^{(0)}$	$A^{(1)}$	$A^{(2)}$	$A^{(1)}$	$A^{(2)}$	$\eta^{(0)}$	$\eta^{(1)}$	$\eta^{(2)}$
x $\xi$	0.1467	-0.1211	0.0274	0.1853	-0.0608	7.0	0.0217	0.0037
xG	2.4120	-1.9845	0.4443	3.6363	-1.4146	5.0	1.5464	-0.5287

	$\eta^{(0)}$	$\eta^{(1)}$	$\eta^{(2)}$	B <sup>(1)</sup>	B <sup>(2)</sup>	C <sup>(0)</sup>	C <sup>(1)</sup>	C <sup>(2)</sup>
x $\xi$	9.5041	1.0165	-0.1049	0.1682	0.4473	25.8997	3.9572	1.6331
xG	13.8237	0.7914	-0.2873	7.6609	-1.4595	36.7928	12.5884	-1.1536

Table I. Values for the parameters defined by Eqs. (5.5a-f) for the Owens-Reya parametrizations of the sea and gluon parton distributions.

## FIGURE CAPTIONS

- Fig. 1: Order  $e^2$  diagrams for  $A(\ell N \rightarrow \ell + X_{\text{col}})$ . Coupling constants at respective vertices are shown in parentheses.
- Fig. 2: Diagrams for  $F_i^{\text{col}}$ . One must sum over the relevant types of partons.
- Fig. 3: Diagrams for  $P_{qq}$ . Solid lines represent quarks, wavy lines represent the probe, and curly lines represent gluons.
- Fig. 4: Diagram for  $P_{Gq}$ .
- Fig. 5: Diagrams for  $P_{qG}$ .
- Fig. 6: Diagrams for  $P_{GG}$ .
- Fig. 7: (a-f) Proton flavor structure function  $F_2^{\text{P,flav}}(x, Q^2)$  vs.  $Q^2$  at  $x = 0.05882, 0.10, 0.22222, 0.28571, 0.40,$  and  $0.66667$ , respectively, calculated using Owens-Reya parton distributions both with charm (solid lines) and without charm (dotted lines), and using the phenomenological formula (dashed lines) of Gordon et al. (Ref. 26). Data points are from Gordon et al.
- Fig. 8: (a-e)  $F_2$  per nucleon for an isoscalar target at  $x = 0.11, 0.16, 0.21, 0.26,$  and  $0.33$ , respectively, assuming  $M_{\text{col}} = 9$  GeV. The solid curves are the usual QCD result and the dashed curves include the contribution from  $F_2^{\text{col}}$ . The data points are from Ball et al. (see Ref. 3).
- Fig. 9: (a-g) Percentage increase in  $F_2$  above the conventional QCD prediction for  $x = 0.03, 0.04, 0.05, 0.10, 0.15, 0.20,$  and  $0.25$ , respectively, and  $M_{\text{col}} = 9$  (solid line), 11 (dashed line), 15 (dotted line), and 20 (dash-dotted line) GeV.

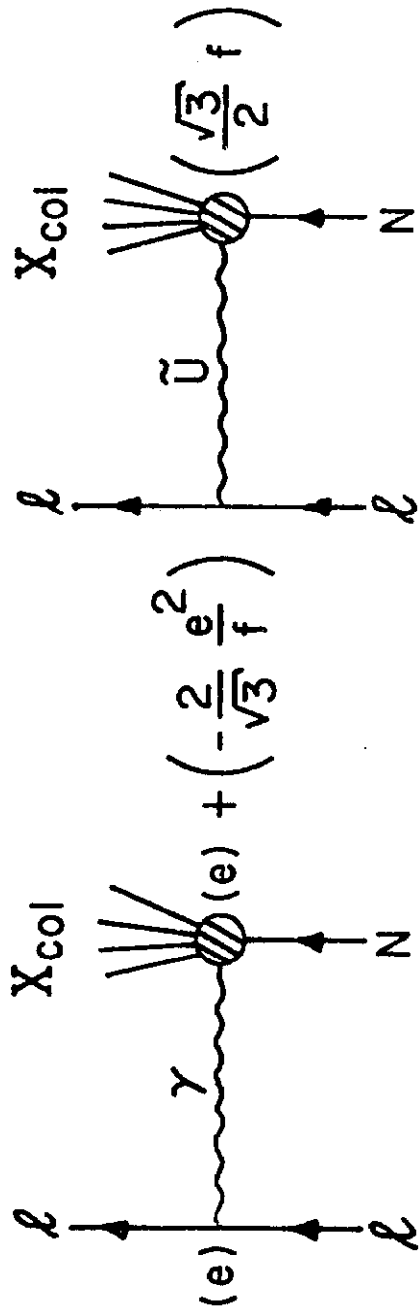


Fig. 1

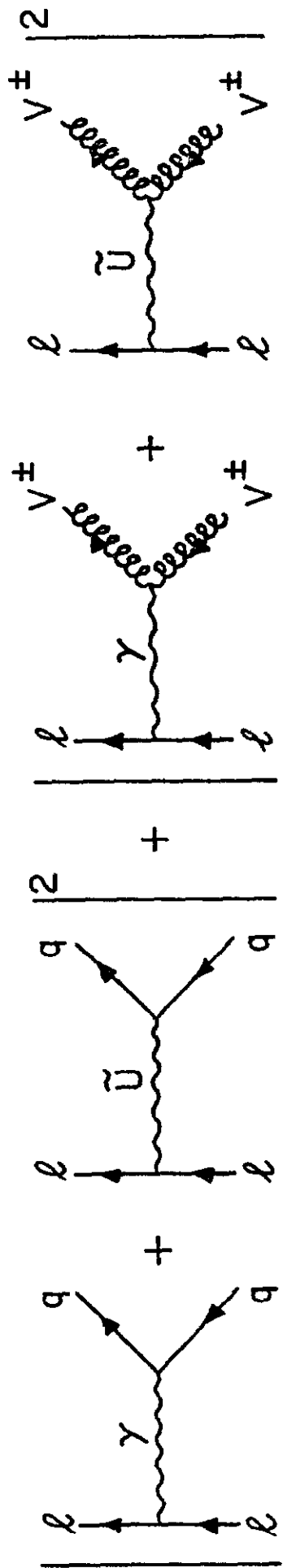


Fig. 2

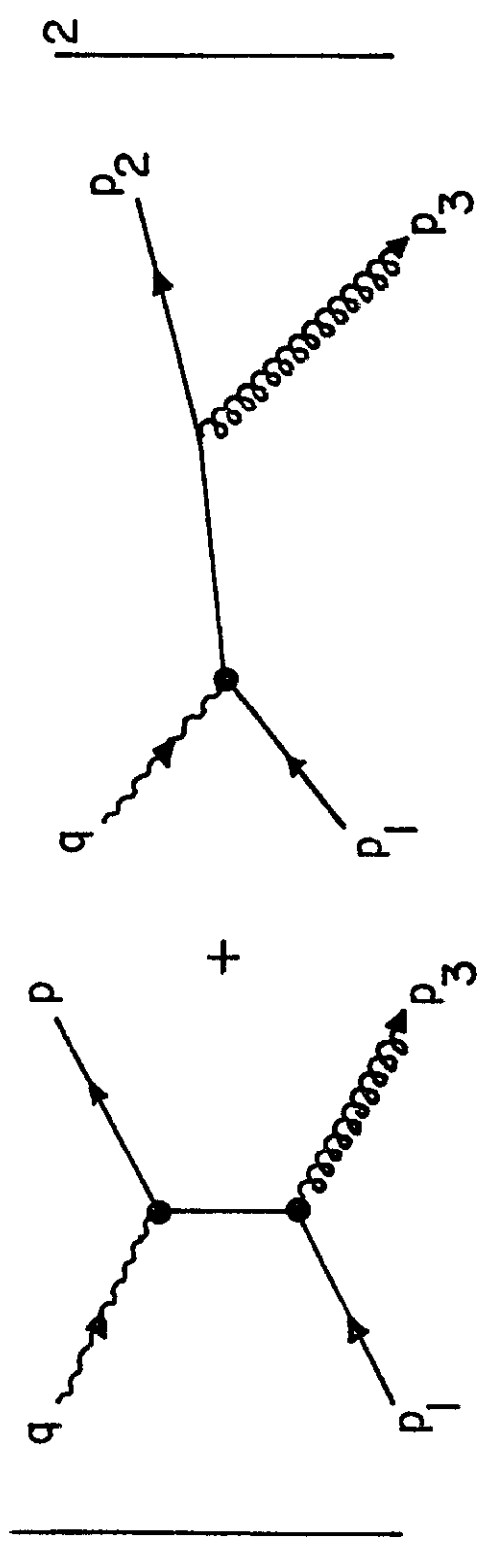
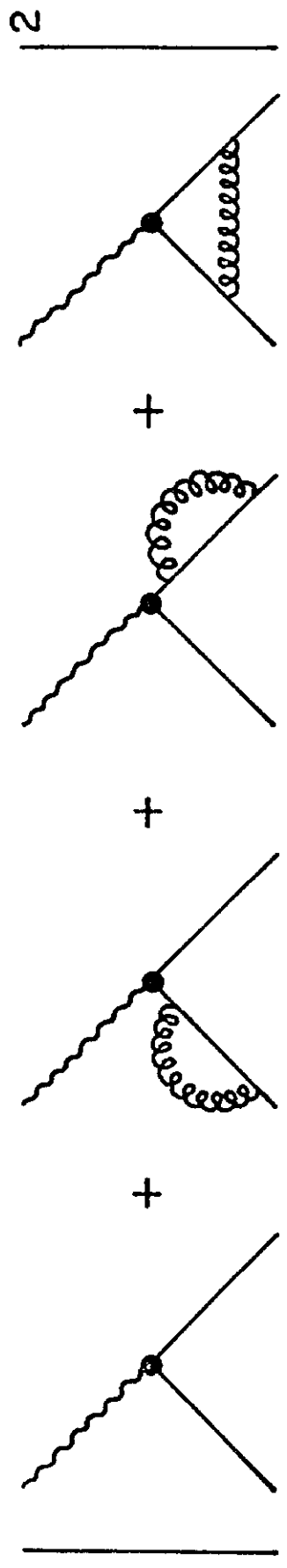


Fig. 3

2, 3



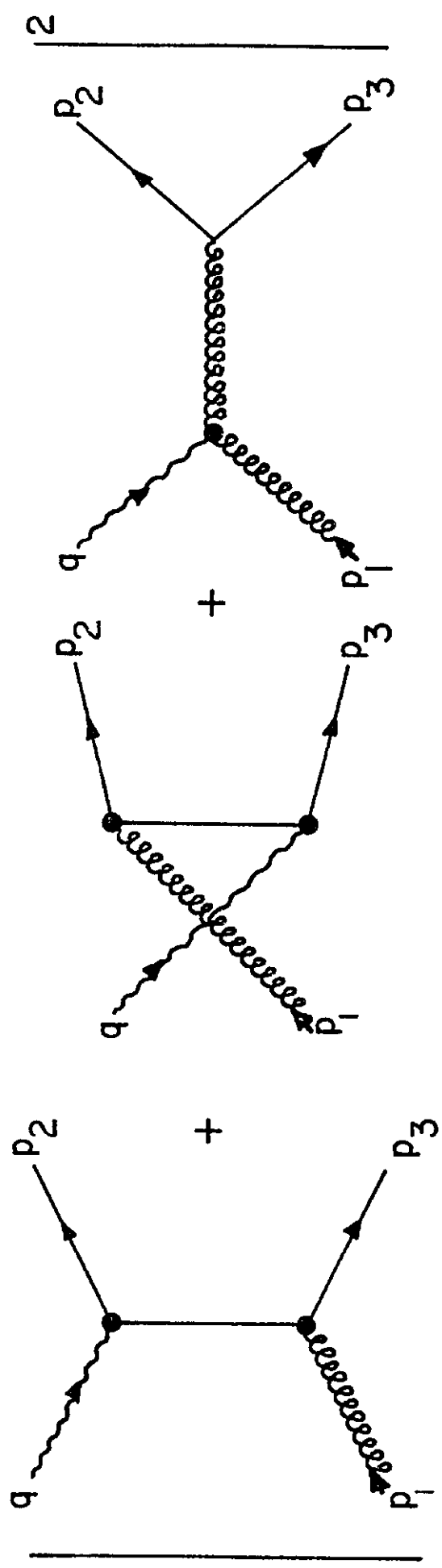


Fig. 5

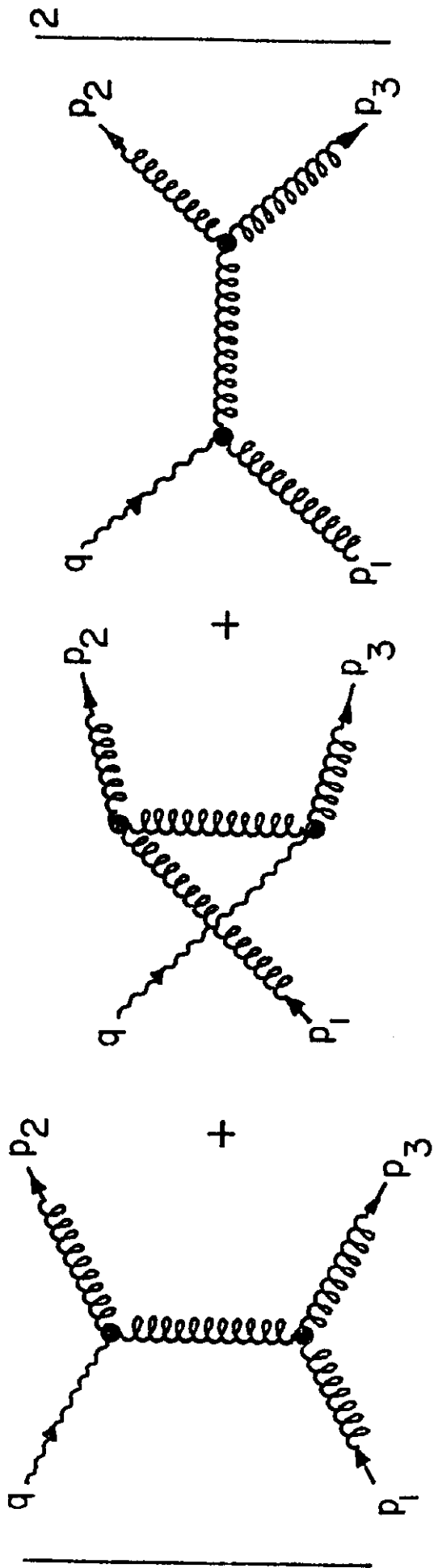


Fig. 6

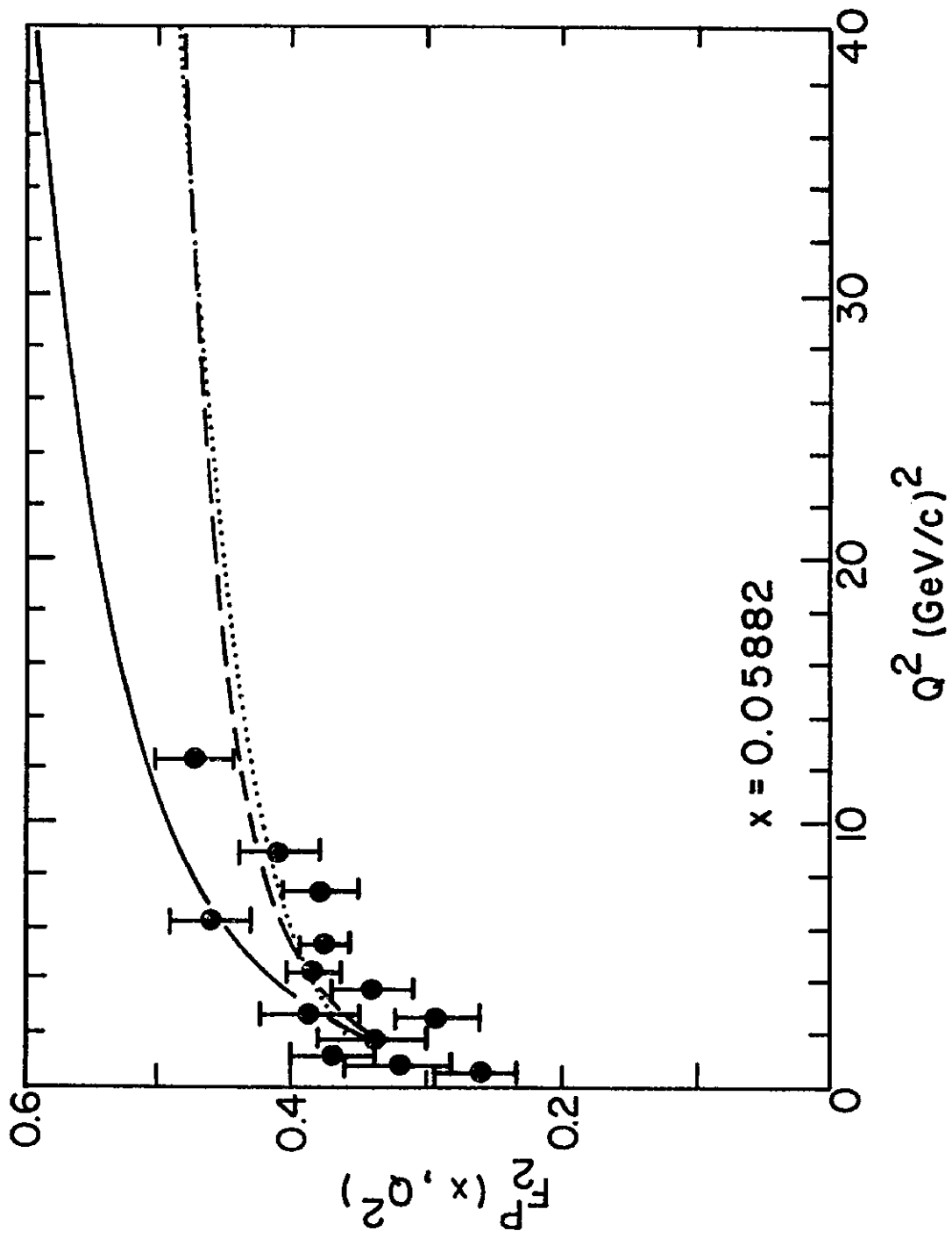


Fig. 7a

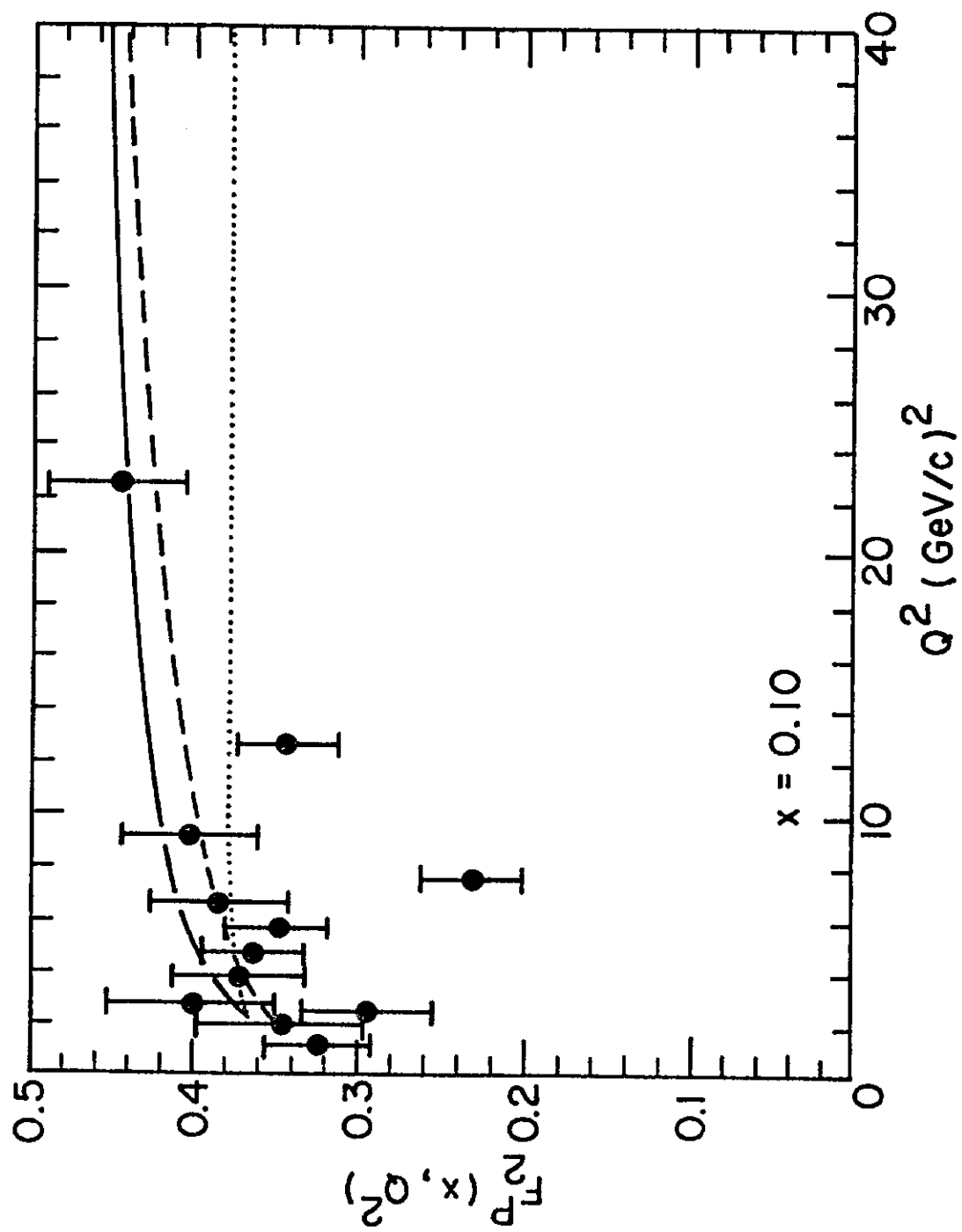


Fig. 7b

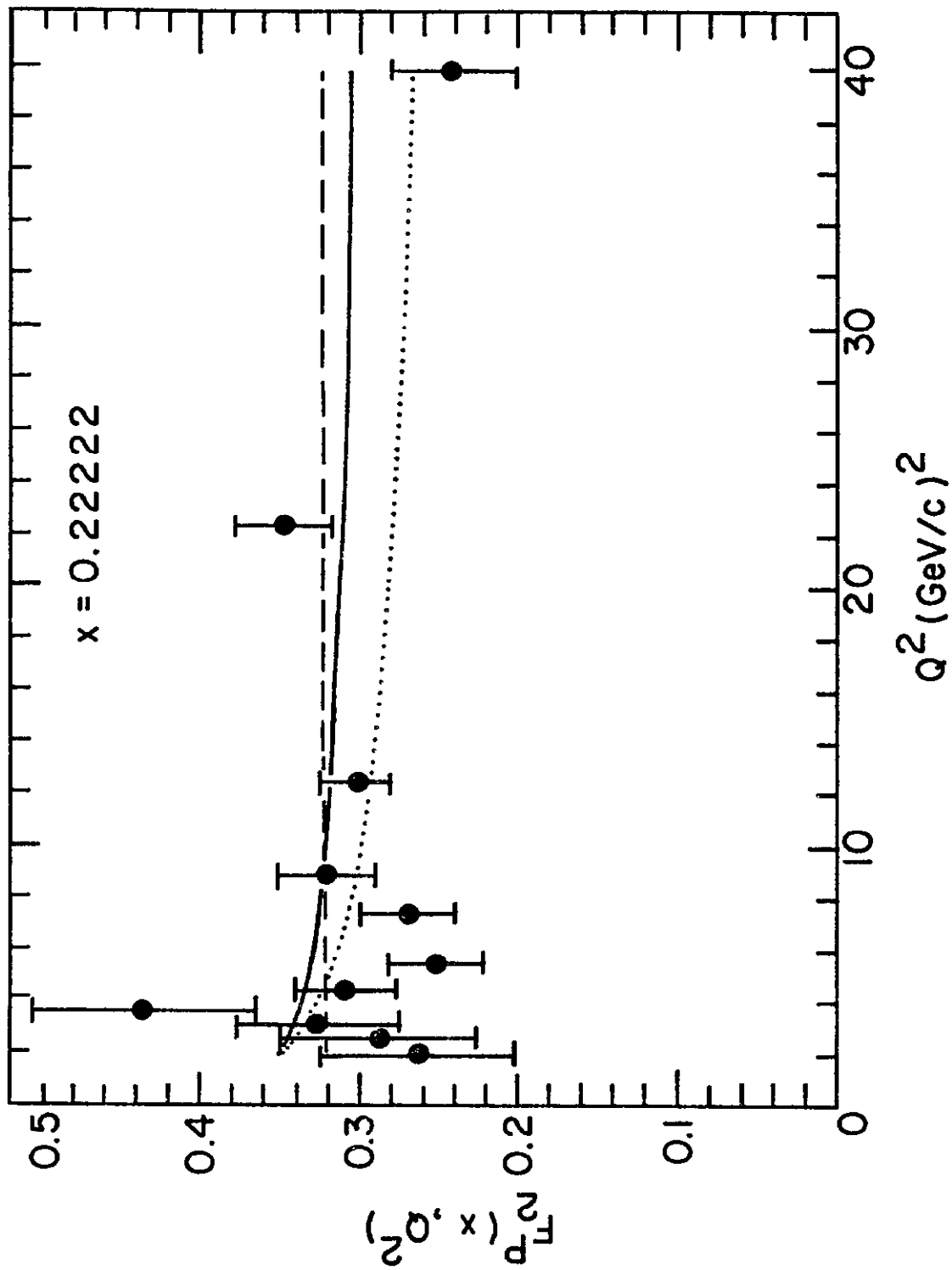


Fig. 7c

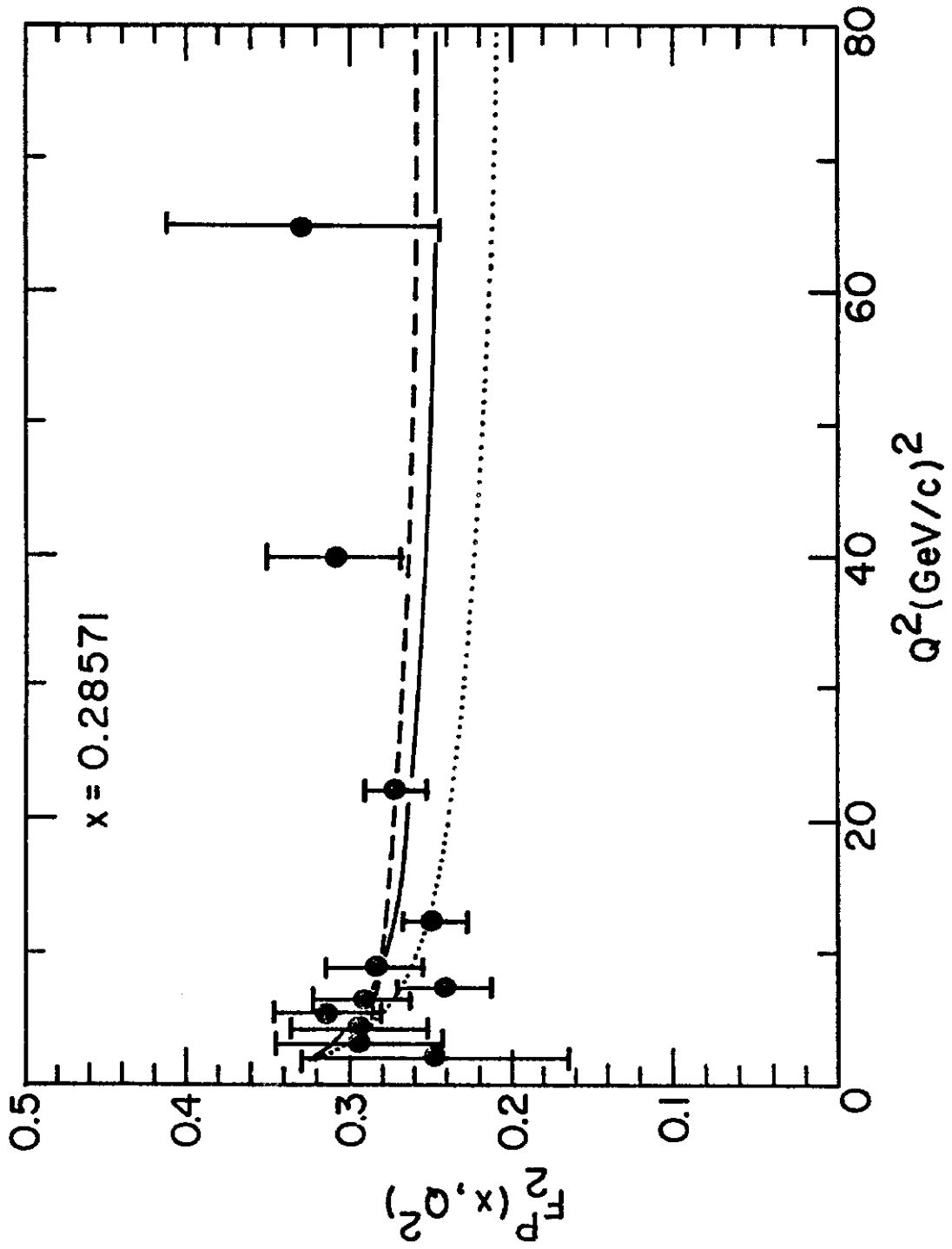


Fig. 7d

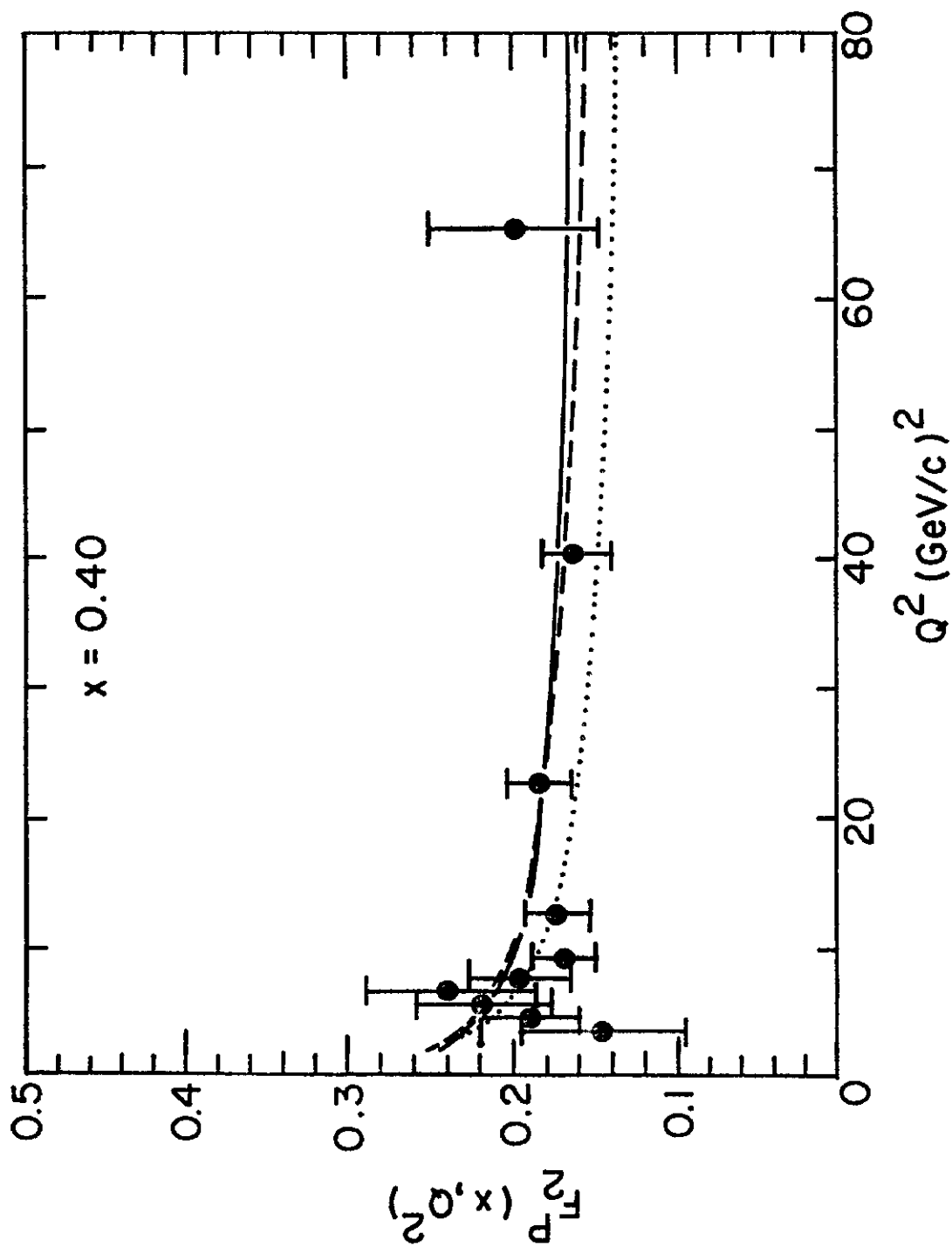


Fig. 7e

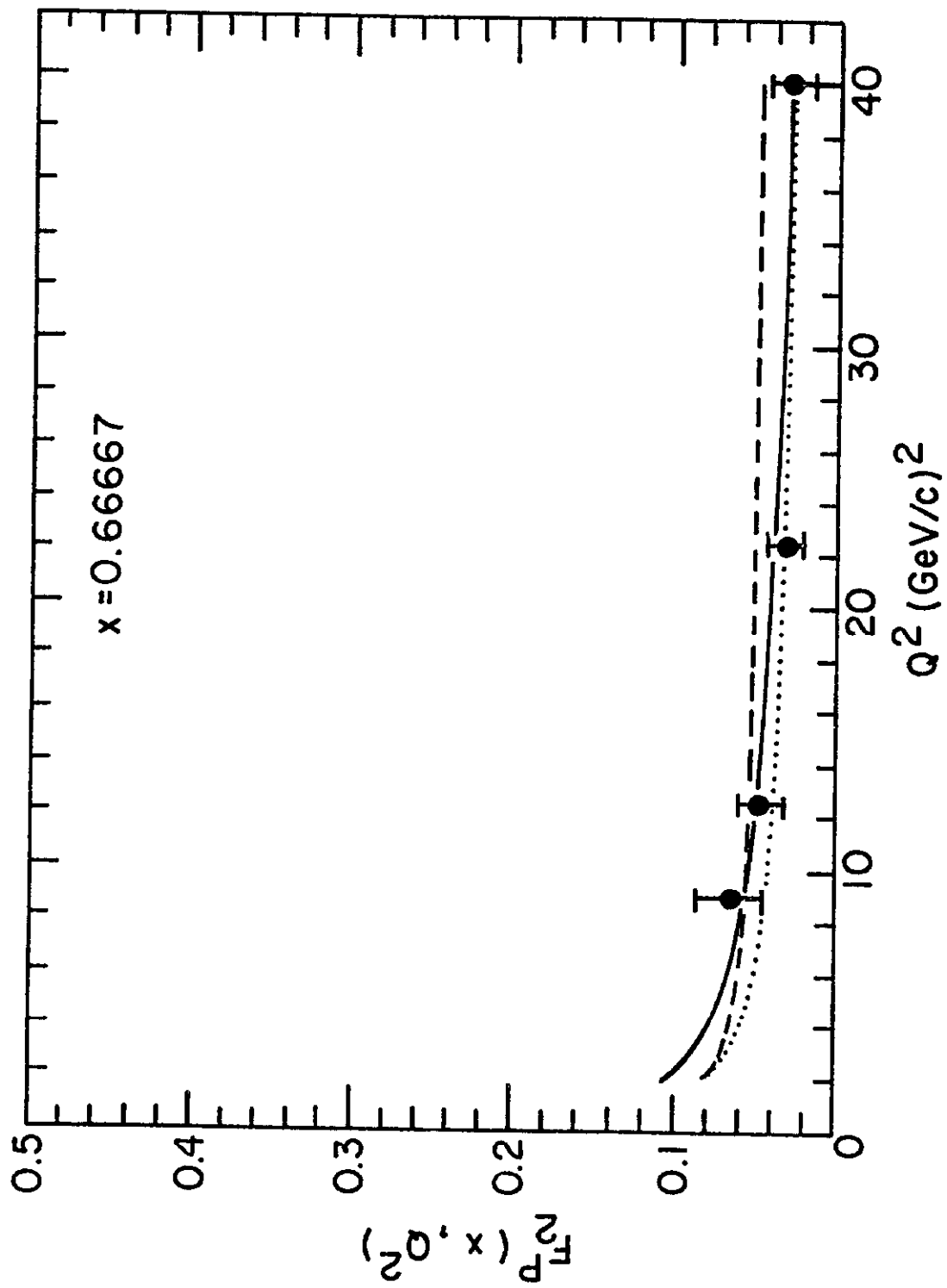


Fig. 7f

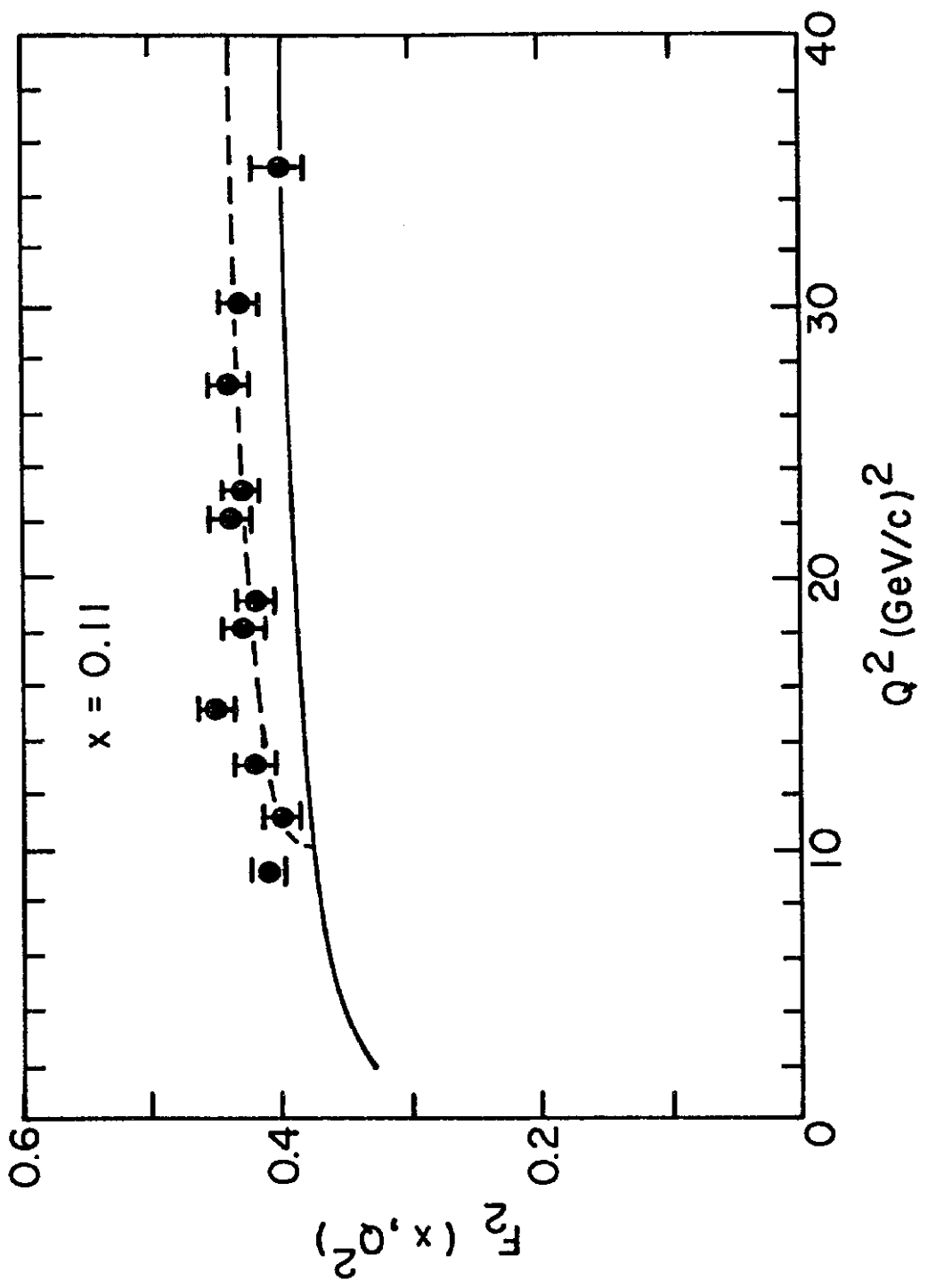


Fig. 8a

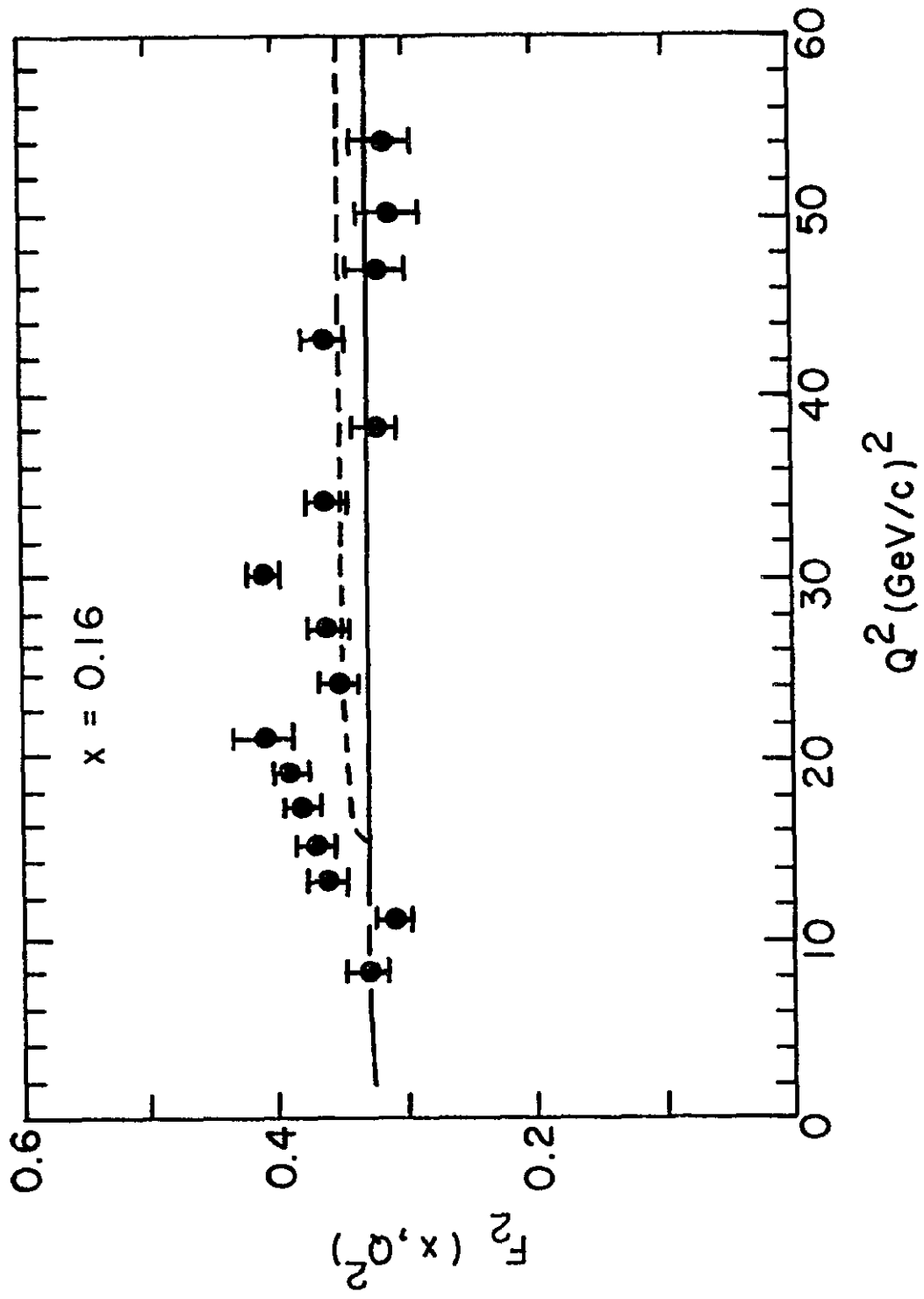


Fig. 8b

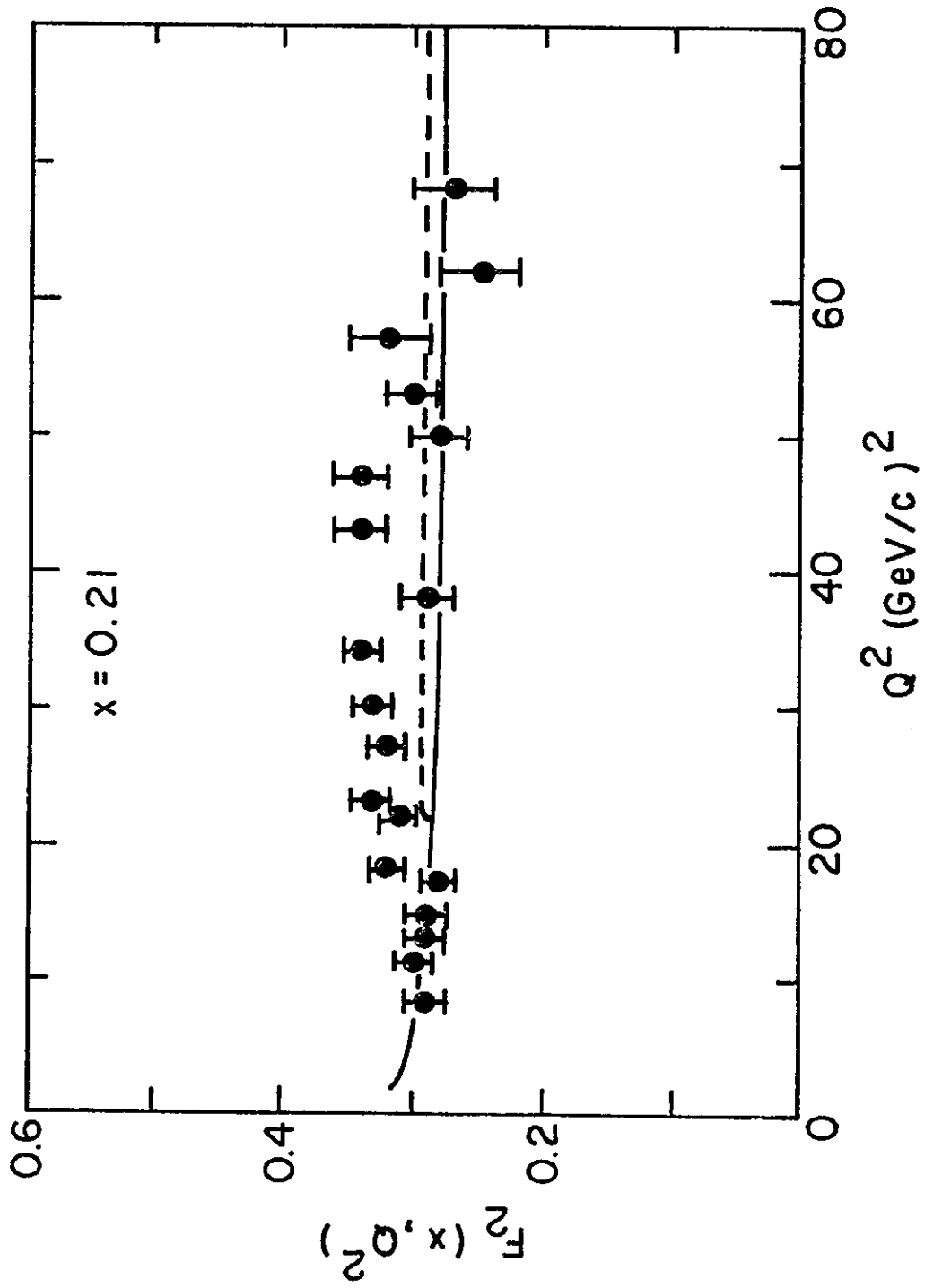


Fig. 8c

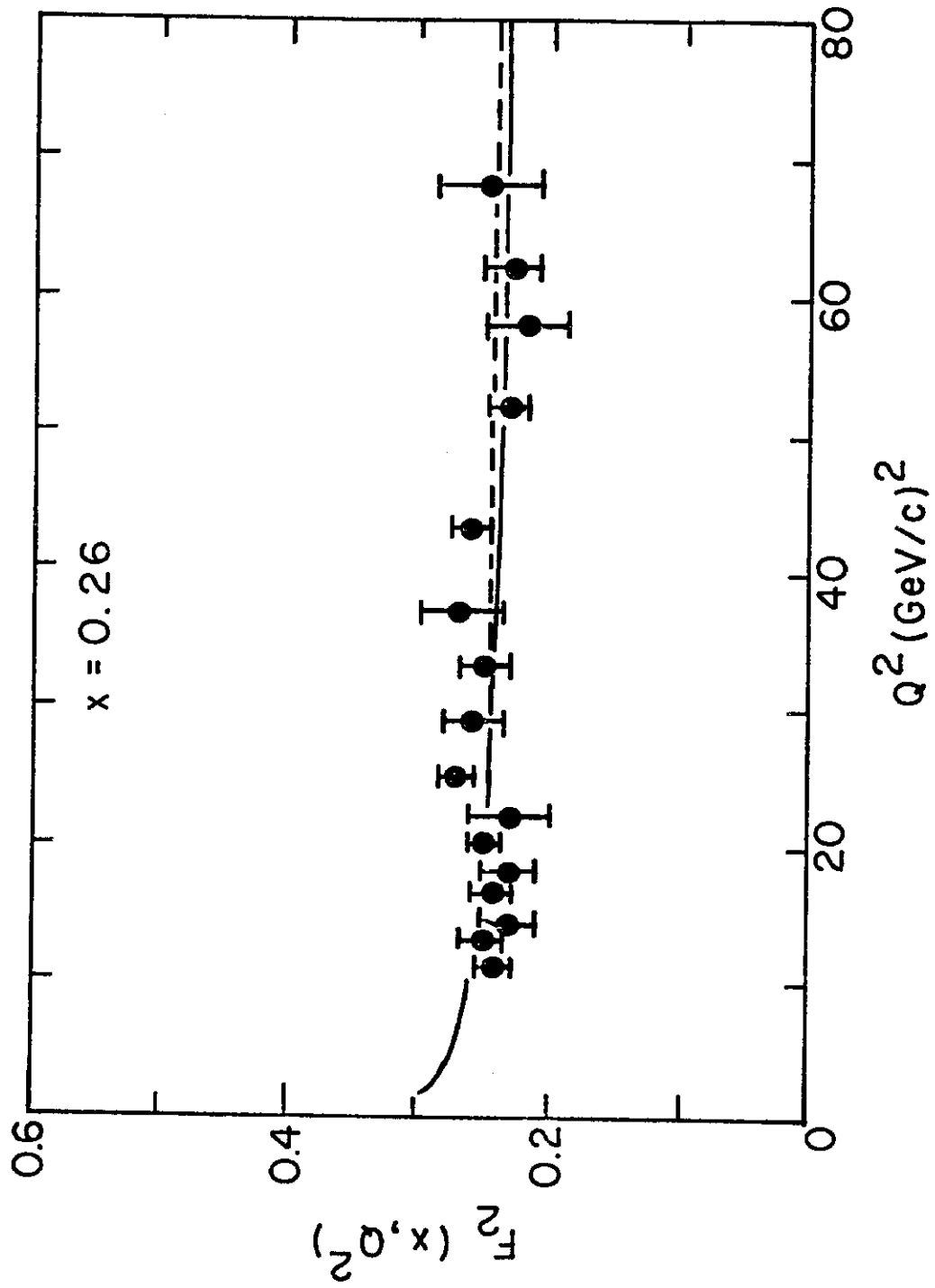


Fig. 8d

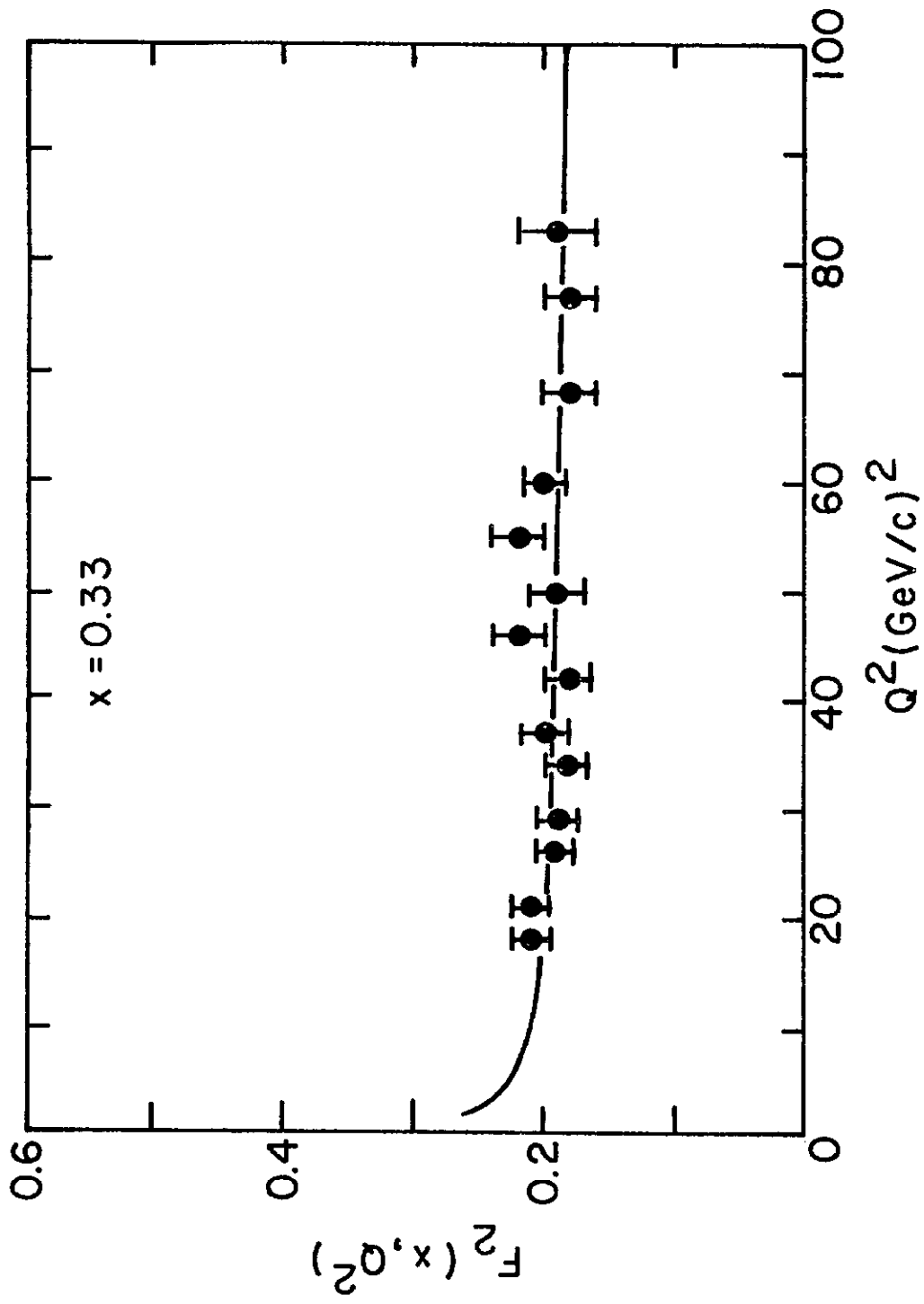


Fig. 8e

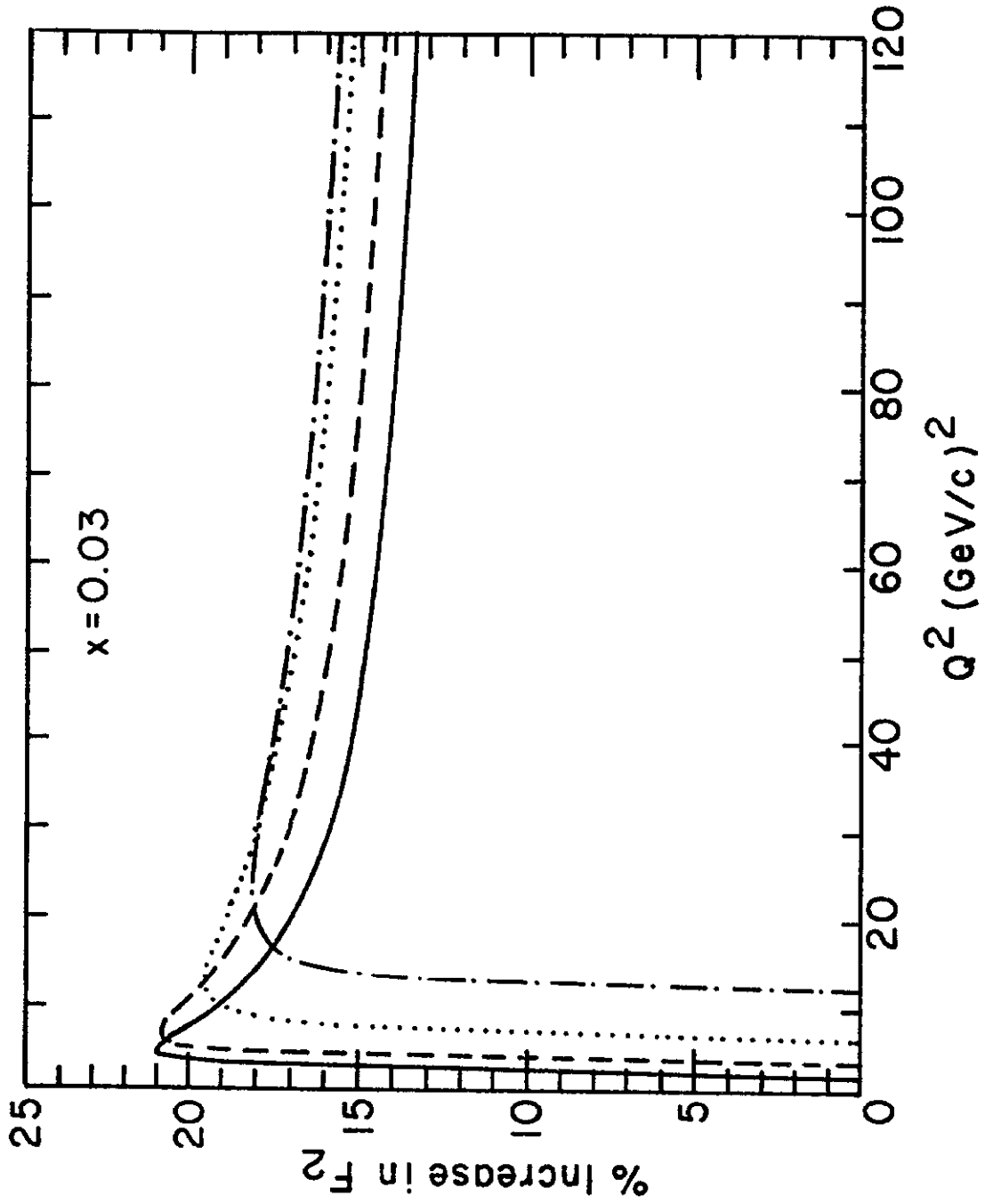


Fig. 9a

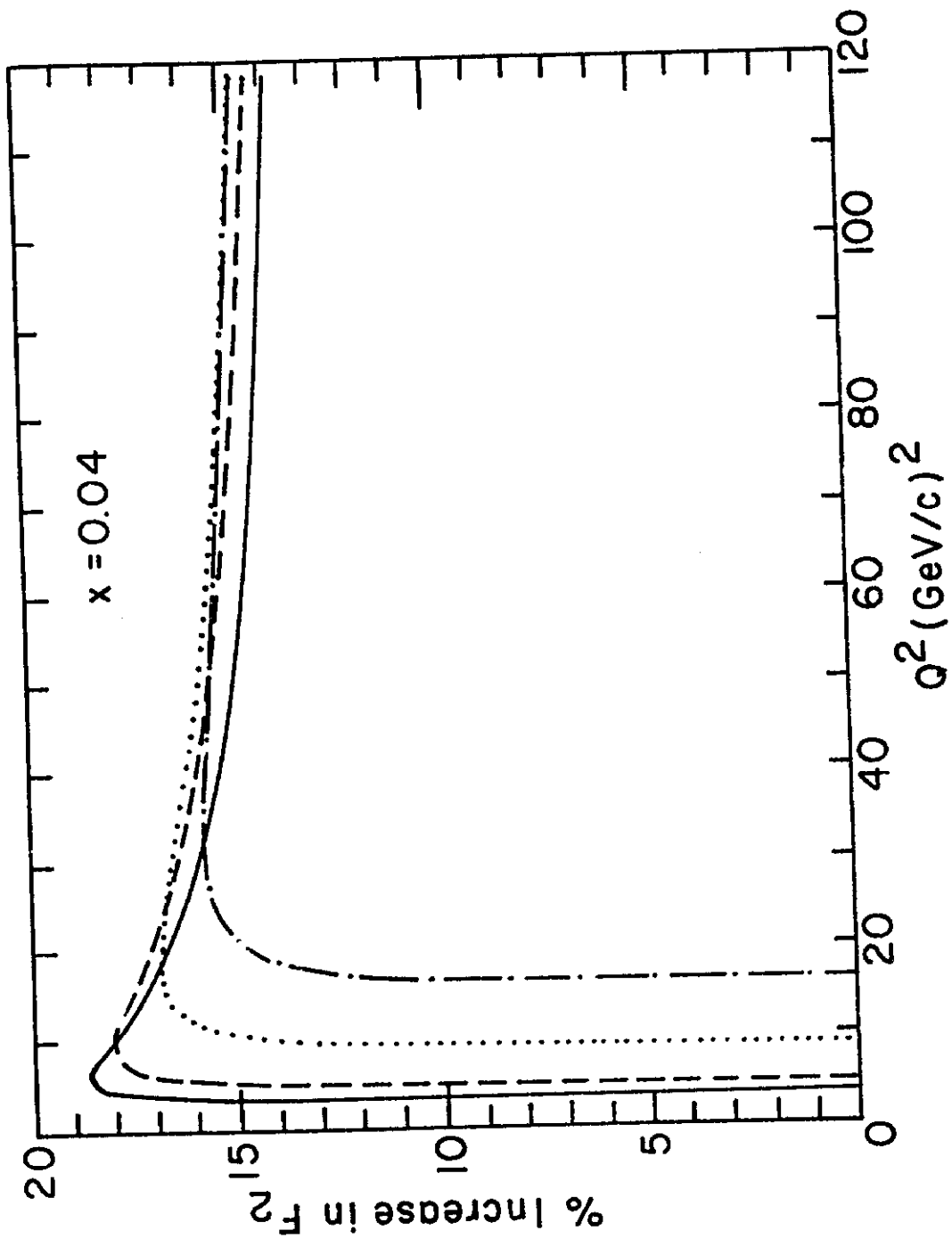


Fig. 9b

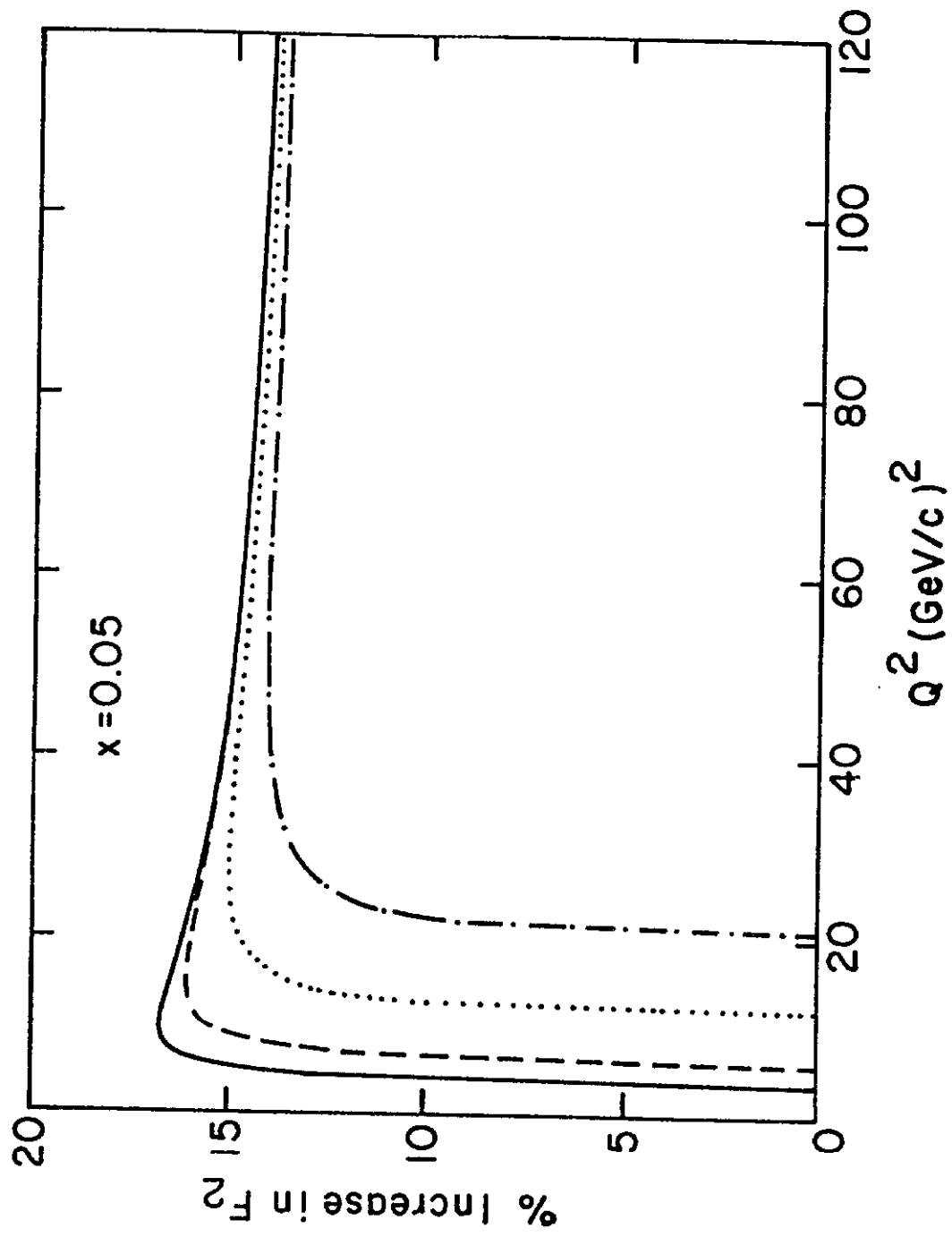


Fig. 9c

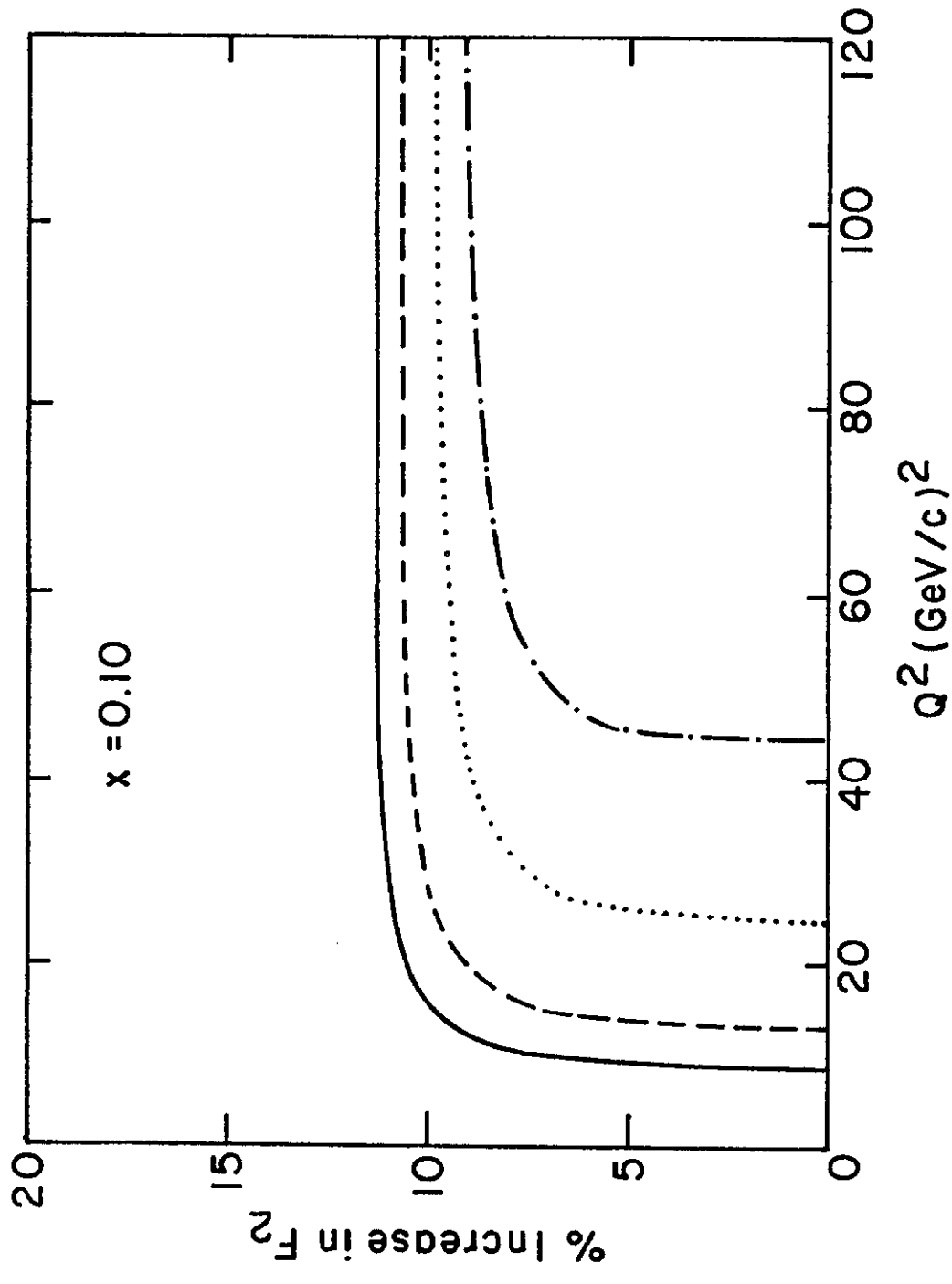


Fig. 9d

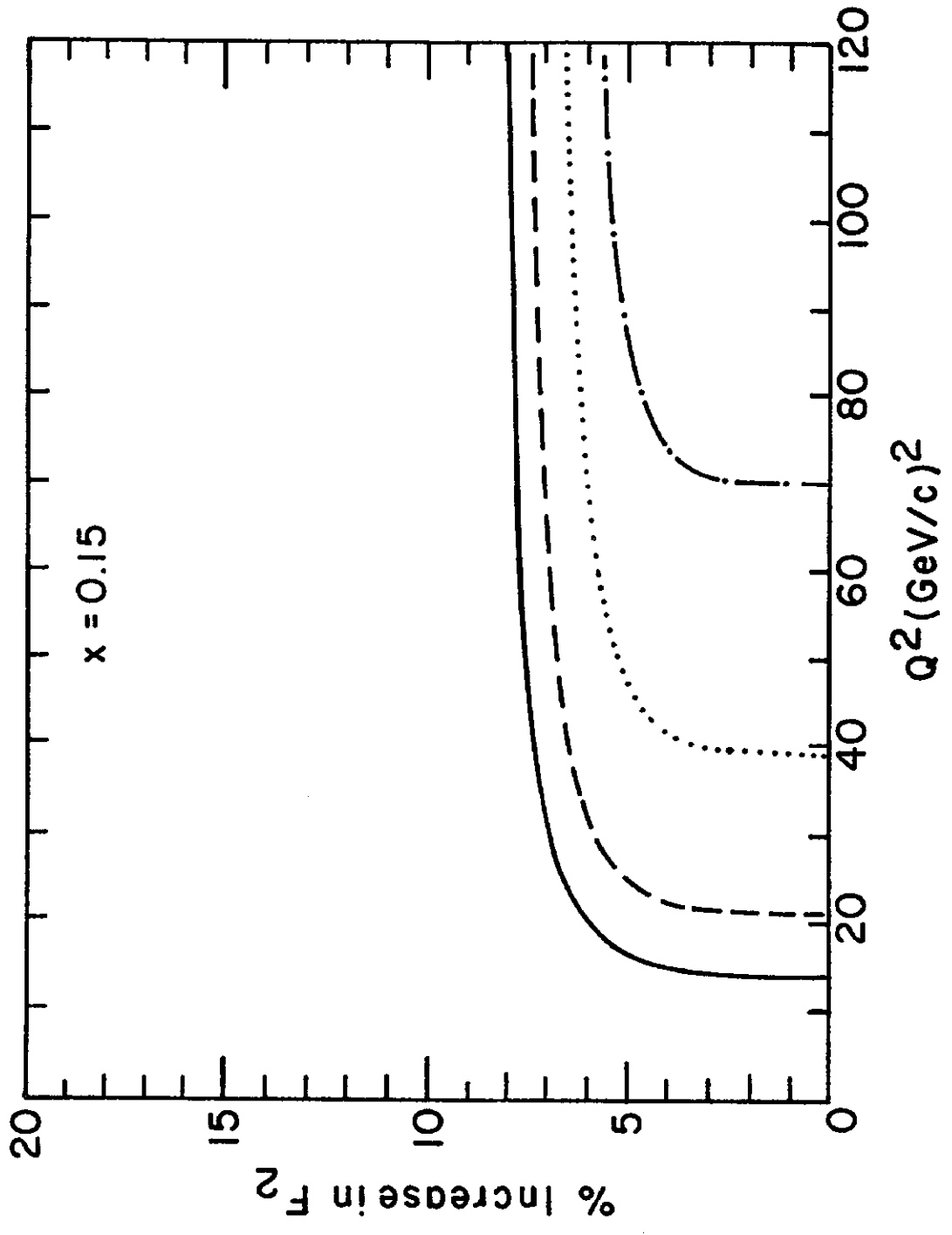


Fig. 9e

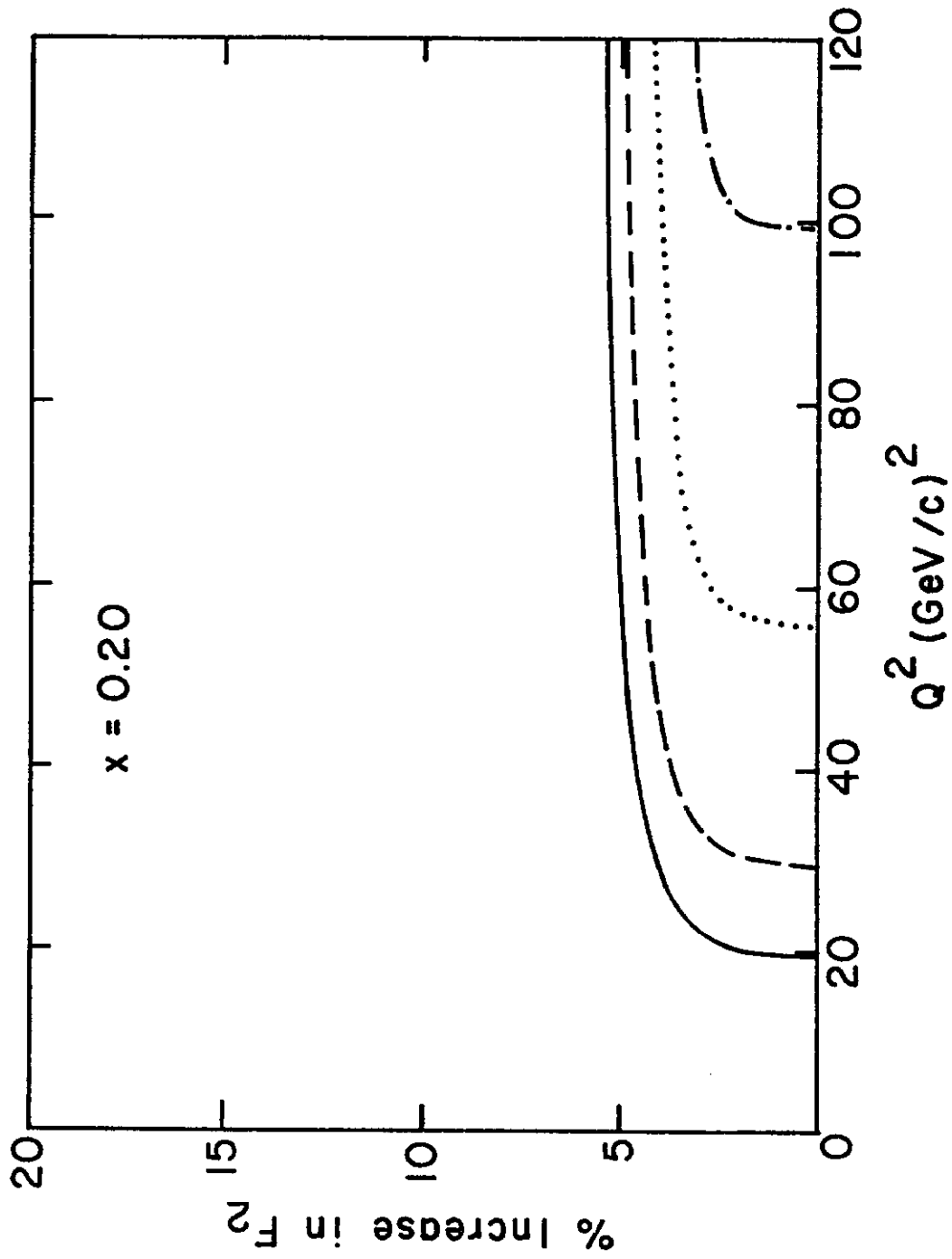


Fig. 9f

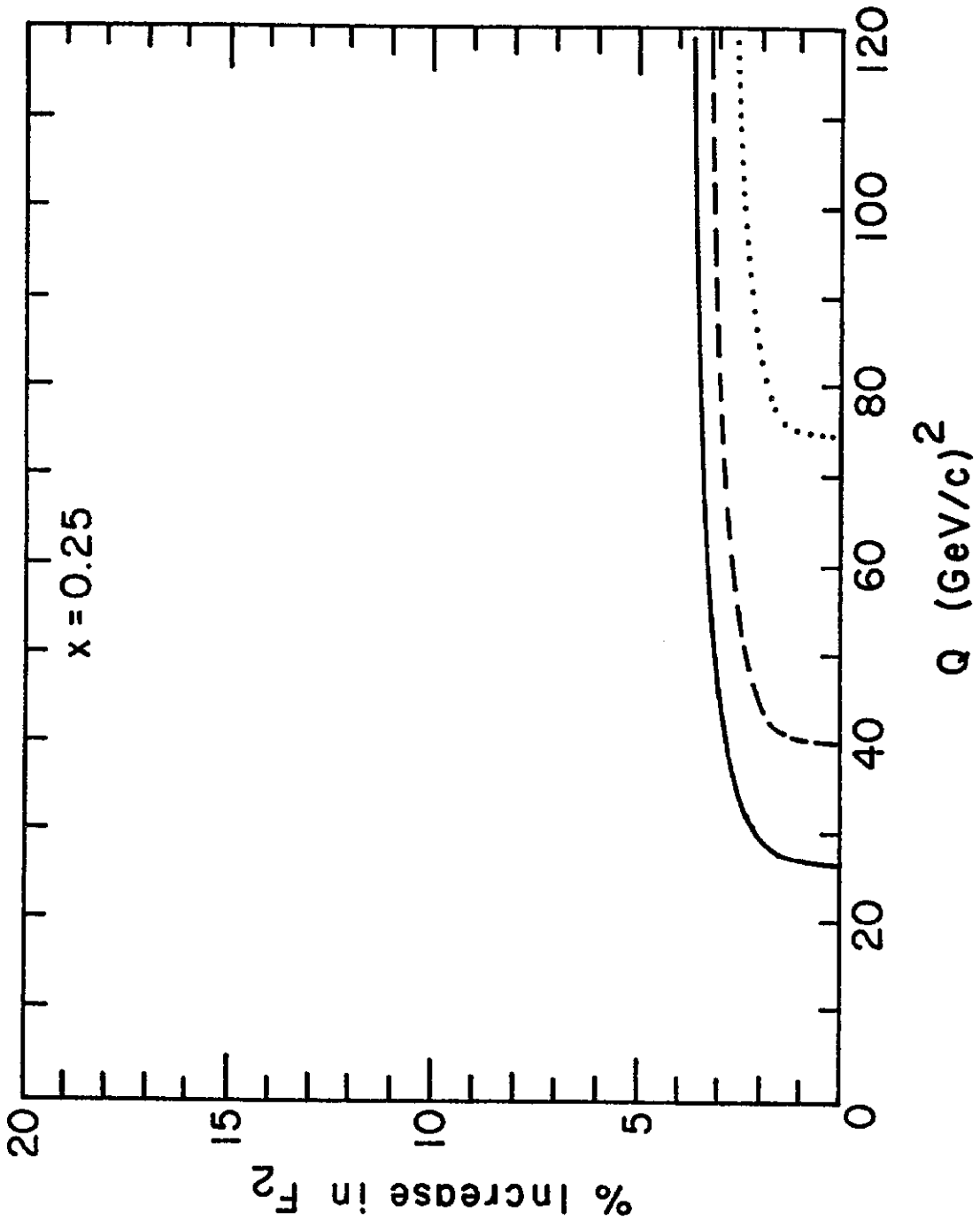


Fig. 98